



Search for a standard model-like Higgs boson in the mass range between 70 and 110 GeV in the diphoton final state in proton-proton collisions at $\sqrt{s} = 8$ and 13 TeV

The CMS Collaboration*

Abstract

The results of a search for a standard model-like Higgs boson in the mass range between 70 and 110 GeV decaying into two photons are presented. The analysis uses the data set collected with the CMS experiment in proton-proton collisions during the 2012 and 2016 LHC running periods. The data sample corresponds to an integrated luminosity of 19.7 (35.9) fb^{-1} at $\sqrt{s} = 8$ (13) TeV. The expected and observed 95% confidence level upper limits on the product of the cross section and branching fraction into two photons are presented. The observed upper limit for the 2012 (2016) data set ranges from 129 (161) fb to 31 (26) fb. The statistical combination of the results from the analyses of the two data sets in the common mass range between 80 and 110 GeV yields an upper limit on the product of the cross section and branching fraction, normalized to that for a standard model-like Higgs boson, ranging from 0.7 to 0.2, with two notable exceptions: one in the region around the Z boson peak, where the limit rises to 1.1, which may be due to the presence of Drell–Yan dielectron production where electrons could be misidentified as isolated photons, and a second due to an observed excess with respect to the standard model prediction, which is maximal for a mass hypothesis of 95.3 GeV with a local (global) significance of 2.8 (1.3) standard deviations.

Published in Physics Letters B as doi:10.1016/j.physletb.2019.03.064.

1 Introduction

Within the standard model (SM) of particle physics [1–3], particle masses arise from the spontaneous breaking of electroweak symmetry, which is achieved through the Brout–Englert–Higgs mechanism [4–9]. In its minimal version, electroweak symmetry breaking is realized through the introduction of a doublet of complex scalar fields. At the end of the process, only one scalar field remains and the corresponding quantum, the Higgs boson, should be experimentally observable. In 2012, both the ATLAS [10] and CMS [11, 12] Collaborations observed a new boson with a mass of approximately 125 GeV whose properties are at present compatible with those of the SM Higgs boson. The analyses of data in the diphoton final state leading to this discovery probed an invariant mass range extending from 110 to 150 GeV.

However, physics beyond the SM (BSM) can also provide a Higgs boson that is compatible with the observed 125 GeV boson. The extended parameter space of several BSM models, for example generalized models containing two Higgs doublets (2HDM) [13–17] and the next-to-minimal supersymmetric model (NMSSM) [18–37], gives rise to a rich and interesting phenomenology, including the presence of additional Higgs bosons, some of which could have masses below 125 GeV. Such models provide good motivation for extending searches for Higgs bosons to masses as far below $m_H = 110$ GeV as possible, where H refers to an additional Higgs boson which is “SM-like”, meaning that the relative contributions of the production processes are similar to those of the SM.

The $H \rightarrow \gamma\gamma$ decay channel provides a clean final-state topology that allows the mass of a Higgs boson in the search range to be reconstructed with high precision. The primary production mechanism for Higgs bosons in proton-proton (pp) collisions at the CERN LHC is gluon fusion (ggH), with additional smaller contributions from vector boson fusion (VBF) and production in association with a W or Z boson (VH), or with a $t\bar{t}$ pair ($t\bar{t}H$). The dominant sources of background are irreducible direct diphoton production, and the reducible $pp \rightarrow \gamma + \text{jet}$ and $pp \rightarrow \text{jet} + \text{jet}$ processes, where the jets are misidentified as isolated photons. An additional source of reducible background relevant for the search range below $m_H = 110$ GeV is Drell–Yan dielectron production, where electrons could be misidentified as isolated photons.

The CERN LEP collaborations [38], in the context of the search for the SM Higgs boson, explored the mass range below 110 GeV extensively in the VH production modes, in the $b\bar{b}$ and $\tau^+\tau^-$ channels. Several of the BSM models mentioned above predict reduced decay rates in these channels with respect to SM predictions and enhanced decay rates in the diphoton channel. The “low-mass” search in the diphoton decay channel by ATLAS [39], performed in the mass range of $65 < m_{\gamma\gamma} < 110$ GeV at a center-of-mass energy of 8 TeV, found no significant excess with respect to expectations.

This letter presents the result of a search in the diphoton channel for an additional Higgs boson with an invariant mass lower than 110 GeV, whose natural width is small compared to the detector resolution. The search is performed on a data set collected in 2012 and 2016 with the CMS detector at the LHC, corresponding to, respectively, integrated luminosities of 19.7 fb^{-1} at a center-of-mass energy of 8 TeV, referred to as the “8 TeV data”, and 35.9 fb^{-1} at 13 TeV, the “13 TeV data”.

The analysis is based on a search for a localized excess in the diphoton invariant mass spectrum over a smoothly falling background from prompt diphoton production and from events with at least one jet misidentified as a photon, in addition to the Drell–Yan contribution. It uses an extended version of the method developed by the CMS Collaboration for the observation and the measurement of the properties of the 125 GeV boson [40, 41]. The invariant mass range

explored in the 8 (13) TeV data is $80 (70) < m_{\gamma\gamma} < 110$ GeV. The principal challenges associated with a search in the diphoton decay channel in this mass range are the ability to trigger on events while maintaining acceptable rates, and the background from Z bosons decaying to electron pairs that, through misidentification, could appear to result in two isolated photons. To achieve the best possible sensitivity, the events are separated into classes. Multivariate analysis (MVA) techniques are used both for photon identification and event classification, and the signal is extracted from the background using a fit to the diphoton mass spectrum in all event classes.

2 The CMS detector

A detailed description of the CMS detector, together with a definition of the coordinate system used and the relevant kinematic variables, can be found in Ref. [42]. The central feature of the CMS apparatus is a superconducting solenoid of 6 m internal diameter, providing a magnetic field of 3.8 T. Within the solenoid volume are a silicon pixel and strip tracker, a lead tungstate crystal electromagnetic calorimeter (ECAL), and a brass and scintillator hadron calorimeter (HCAL), each composed of a barrel and two endcap sections. Forward calorimeters extend the pseudorapidity (η) coverage provided by the barrel and endcap detectors. Muons are detected in gas-ionization chambers embedded in the steel flux-return yoke outside the solenoid. The ECAL, surrounding the tracker volume, consists of 75 848 lead tungstate crystals, which provide coverage in $|\eta| < 1.48$ in a barrel region (EB) and $1.48 < |\eta| < 3.0$ in two endcap regions (EE). Preshower detectors consisting of two planes of silicon sensors interleaved with a total of $3X_0$ of lead are located in front of each EE detector. In the EB, an energy resolution of about 1% is achieved for unconverted or late-converting photons that have energies in the range of tens of GeV. For the remaining barrel photons, a resolution of about 1.3% is achieved up to $|\eta| = 1$, rising to about 2.5% at $|\eta| = 1.4$. In the EE, an energy resolution for unconverted or late-converting photons of about 2.5% is achieved, while for the remaining endcap photons it is between 3 and 4% [43].

3 Measurement of the diphoton mass spectrum

3.1 Trigger and simulation

Events of interest are selected using a two-tiered trigger system [44]. The first level, composed of custom hardware processors, uses information from the calorimeters and muon detectors to select events at a rate of around 100 kHz within a time interval of less than 4 μ s. The second level, known as the high-level trigger (HLT), consists of a farm of processors running a version of the full event reconstruction software optimized for fast processing, and reduces the event rate to less than 1 kHz before data storage. For this analysis, diphoton HLT paths with asymmetric transverse momentum (p_T) thresholds are used.

In the case of the 8 TeV data, the same paths are used as in [40]. The paths that select almost all of the events impose thresholds of 26 and 18 GeV on the p_T of the individual photon trigger objects, and minimum requirements on the invariant mass of diphoton trigger objects of either 60 or 70 GeV depending on the data-taking period.

For the 13 TeV data, two dedicated HLT paths are used, both with photon p_T thresholds of 30 and 18 GeV. One path has nearly identical requirements to those used in [41], except that only events with both photon candidates in the EB are selected. This path requires each of the photon candidates to satisfy criteria on the ratio of its energy in the HCAL and in the ECAL (H/E), and

on either shower shape or on its isolation energy. The other path selects events with photon candidates from any part of the ECAL, but they must satisfy more stringent shower shape requirements as well as the requirements on both isolation energy and H/E. In addition, both paths impose a veto on the presence of hits compatible with the photon direction in the silicon pixel detector, and require that the invariant mass of the two photon candidates be greater than 55 GeV.

These requirements limit the search range to $m_{\gamma\gamma} > 70$ (80) GeV for the 13 (8) TeV data, in order to avoid the portion of the offline diphoton spectrum that is distorted due to turn-on effects from the HLT criteria. For both data sets, the trigger efficiency is measured from $Z \rightarrow e^+e^-$ events using the tag-and-probe technique [45], except for the pixel hit veto requirement relevant for the triggering of the 13 TeV data, where the efficiency is measured using diphoton events in data that have passed the trigger used in [41], which does not require a pixel veto.

Monte Carlo (MC) simulations are used to produce SM Higgs boson events from all production processes (ggH, VBF, VH, and ttH), with invariant masses ranging from 70 to 110 GeV. These events are the input to the signal modeling procedure, representing a new resonance decaying to two photons. In the case of the 8 TeV data, for the ggH and VBF processes, these events are generated at next-to-leading order (NLO) in perturbative quantum chromodynamics (QCD) using POWHEG 1.0 [46–50], while the events from the associated production processes are generated at leading order (LO) with PYTHIA 6.426 [51]. For the 13 TeV data, events are generated at NLO using MADGRAPH5_aMC@NLO 2.2.2 [52] with FxFx merging [53], for all production processes. Events generated at LO (NLO) for the analysis of the 8 TeV data use the CTEQ6L [54] (CTEQ6M [55]) set of parton distribution functions (PDFs), while those intended for the analysis of the 13 TeV data use the NNPDF3.0 [56] PDF set. The parton-level samples are interfaced to PYTHIA 6.426 for the 8 TeV data, and to PYTHIA 8.205 [57] for the 13 TeV data for parton showering and hadronization, with the Z2* [58, 59] and CUETP8M1 [59] tune parameter sets used, respectively, for the underlying event activity. The cross sections and branching fractions recommended by the LHC Higgs cross section working group for center-of-mass energies of 8 and 13 TeV [60] are assumed. After the generation step, the events are processed by the full CMS detector simulation with GEANT4 [61]. Multiple pp interactions in each bunch crossing in each recorded event (pileup) are simulated. These events are then weighted to reproduce the distribution of the number of interactions observed in data in 2012 (2016) for the 8 (13) TeV data, the average values of which were 21 and 23 interactions, respectively. The trigger efficiencies measured using the method described above are applied to the simulated SM Higgs boson events as a correction, and the associated statistical and systematic uncertainties are propagated to the expected signal yields.

Events corresponding to the SM background processes mentioned in Section 1 are simulated using various generators. The diphoton background is modeled with the SHERPA 1.4.2 (2.2.0) [62] generator for the analysis of the 8 (13) TeV data; it includes the Born processes with up to 2 (3) additional jets, as well as the box processes at LO. Multijet and $\gamma + \text{jet}$ backgrounds are modeled with PYTHIA 6.426 (8.205) in the case of the 8 (13) TeV data, with a filter [40, 41] applied at generator level in order to enhance the production of jets with a large fraction of electromagnetic energy. Drell–Yan events are simulated at LO with MADGRAPH5 1.3.30 [52] and at NLO with POWHEG 1.0 [63] in the case of the 8 TeV data, and entirely at NLO with MADGRAPH5_aMC@NLO 2.2.2 for the 13 TeV data. All background events are generated using the same PDF sets and simulated under the same conditions as the SM Higgs boson events described above. The background events are used in the calculation of energy scale and smearing corrections, preselection and photon identification efficiencies, training of the multivariate boosted decision trees (BDTs) used in the analysis, estimations of systematic uncertainties, and

for validation. In particular, the Drell–Yan events are used to obtain initial values for some of the parameters used to model the shape of the small background contribution from dielectron decays of the Z boson, which can be misidentified as photon pairs. As in [40] and [41], the background estimation is extracted from data.

3.2 Photon reconstruction, event selection and classification

The same diphoton vertex identification is used as in [40] ([41]) for the 8 (13) TeV data. For both data sets, a BDT is used to select a diphoton vertex from the set of all reconstructed primary vertices, incorporating as input variables the sum of the squared transverse momenta of the charged particle tracks associated with the vertex, and two variables that quantify the vector and scalar balance of p_T between the diphoton system and the charged particle tracks associated with the vertex. Furthermore, if either photon is associated with any charged particle tracks that have been identified as resulting from conversion, the pull between the longitudinal positions of the primary vertex obtained from the conversion tracks alone and from all associated tracks is added to the BDT input variable set, and, in the case of the 13 TeV data, the number of conversions.

The same photon reconstruction is used as in [40] ([41]) for the 8 (13) TeV data. For the 8 TeV data, photon candidates are reconstructed from energy deposits in the ECAL grouped into extended clusters or groups of clusters known as “superclusters”. In the EB, superclusters are formed from five-crystal-wide strips in η , centered on the locally most energetic crystal, and have a variable extension in ϕ . In the EE detectors, where the crystals are arranged according to an x – y rather than an η – ϕ geometry, matrices of 5×5 crystals, which may partially overlap and are centered on a locally most energetic crystal, are summed if they lie within a narrow ϕ road. For the 13 TeV data, photon candidates are reconstructed as part of the global event reconstruction, as described in [64]. First, cluster “seeds” are identified as local energy maxima above a given threshold. Second, clusters are grown from the seeds by aggregating crystals with at least one side in common with a clustered crystal and with an energy in excess of a given threshold. This threshold represents approximately two standard deviations of the electronic noise in the ECAL, and amounts to 80 MeV in the EB and, depending on $|\eta|$, up to 300 MeV in the EE detectors. The energy of each crystal can be shared among adjacent clusters assuming a Gaussian transverse profile of the electromagnetic shower. Finally, clusters are merged into superclusters.

For both data sets, the energy of photons is computed from the sum of the energy of the clustered crystals, calibrated and corrected for changes in the response over time [65]. The preshower energy is added to that of the superclusters in the region covered by this detector. To optimize the resolution, the photon energy is corrected for the containment of the electromagnetic shower in the superclusters and the energy losses from converted photons [43]. The correction is computed with a multivariate regression technique that estimates simultaneously the energy of the photon and its uncertainty. This regression is trained on simulated photons using as the target the ratio of the true photon energy and the sum of the energy of the clustered crystals. The inputs are shower shapes and position variables—both sensitive to shower containment and possible unclustered energy—preshower information, and global event observables sensitive to pileup.

Photon candidates are subject to a preselection that imposes requirements on p_T , hadronic leakage, and shower shape, and that uses an electron veto to reject photon candidates geometrically matched to a hit in the pixel detector. The preselection is designed to be slightly more stringent than the trigger requirements. A photon identification BDT combining lateral shower

shape variables, isolation variables, the median energy density, the pseudorapidity, and the raw energy is used to separate prompt photons from nonprompt photons resulting from neutral meson decays [40, 41]. Each photon candidate must satisfy the preselection requirements as well as a requirement on the minimum value of the photon identification BDT output. As in [40, 41], the efficiencies of the minimum photon identification BDT output requirement and preselection criteria (except for the electron veto requirement) are measured with a tag-and-probe technique using $Z \rightarrow e^+e^-$ events. The fraction of photons that satisfy the electron veto requirement is measured with $Z \rightarrow \mu^+\mu^-\gamma$ events, in which the photon is produced by final-state radiation providing a sample of prompt photons with purity higher than 99%. The ratios of the efficiencies in data and simulation are used to correct the signal efficiency in simulated signal samples and the associated statistical and systematic uncertainties are propagated to the expected signal yields.

The analysis uses all events that contain a diphoton pair where each of the photons in the pair satisfy a requirement on the ratio of its p_T value to the invariant mass of the diphoton system, $m_{\gamma\gamma}$. Specifically, in the case of the 8 (13) TeV data, the requirements are $p_T^{\gamma 1}/m_{\gamma\gamma} > 28.0/80.0 = 0.35$ ($30.6/65.0 = 0.47$) and $p_T^{\gamma 2}/m_{\gamma\gamma} > 20.0/80.0 = 0.25$ ($18.2/65.0 = 0.28$). Here, $\gamma 1$ ($\gamma 2$) refers to the photon candidate with the highest (next-highest) p_T value. The use of p_T thresholds scaled by $m_{\gamma\gamma}$ [40, 41] is intended to prevent a distortion of the low end of the diphoton mass spectrum that results if a fixed threshold is used; in particular, the minimum p_T values in the above fractions, 28 (30.6) GeV and 20 (18.2) GeV for the 8 (13) TeV data, are chosen to be slightly higher than those of the HLT paths, i.e., 26 (30) GeV and 18 GeV for the 8 (13) TeV data, to further guard against distortion of the spectrum. Finally, the diphoton system invariant mass must lie within the range 65 (75) $< m_{\gamma\gamma} < 120$ GeV in the case of the 13 (8) TeV data.

A multivariate event classifier [40, 41] is used to discriminate between diphoton events from Higgs boson decays and those from the diphoton continuum, to further reduce background from events containing jets misidentified as isolated photons, and to assign a high score to events with good diphoton mass resolution. It incorporates the kinematic properties of the diphoton system (excluding $m_{\gamma\gamma}$), a per-event estimate of the diphoton mass resolution, and the photon identification BDT output values. The events are separated into classes based on the classifier score, with a minimum score below which they are rejected. The number of classes and their boundaries are determined so as to maximize the expected signal significance. Four (three) classes are used for the 8 (13) TeV data; they are referred to as 0, 1, 2, and 3 (0, 1, and 2), where class 0 contains the events with greatest expected sensitivity. The fraction of events containing more than one diphoton candidate is of order 10^{-4} . In these cases, the candidate assigned to the highest sensitivity class is selected; should this class still contain multiple diphoton candidates, the candidate with the highest value of $p_T^{\gamma 1} + p_T^{\gamma 2}$ is then selected.

4 Signal parametrization

In order to perform a statistical interpretation of the data, it is necessary to have a description of the signal that includes the overall product of the efficiency and acceptance, as well as the shape of the diphoton mass distribution in each of the event classes. The simulated SM Higgs boson events are used to construct a parameterized signal model that is defined continuously for any value of Higgs boson mass between 80 (70) and 110 GeV, for the 8 (13) TeV data. The photon energy resolution predicted by the simulation is modified by a Gaussian smearing determined from the comparison between the $Z \rightarrow e^+e^-$ line-shape in data and simulation, where the electron energies have been corrected with factors developed for photons, using the same procedure as that described in [40, 41]. The amount of smearing is extracted differen-

tially in bins of $|\eta|$ and the R_9 shower shape variable [43], defined as the energy sum of 3×3 crystals centered on the most energetic crystal in the ECAL cluster divided by the energy of the cluster. The trigger and preselection efficiency corrections described in Sections 3.1 and 3.2, respectively, are also applied to the simulated signal events.

Since the shape of the $m_{\gamma\gamma}$ distribution changes considerably depending on whether the vertex associated with the candidate diphoton is correctly identified, separate fits are made to the distributions for the correct and incorrect primary vertex selections when constructing the signal model. Events are considered to have the correct primary vertex if the vertex associated with the candidate diphoton is within 1 cm of the true vertex. For these events the signal shape is dominated by ECAL response and reconstruction, and is modeled empirically by a sum of between three and six (three and four) Gaussian functions in the case of the 8 (13) TeV data, depending on the event class. The signal shape for events with an incorrect primary vertex selection is smeared significantly by the variation in the z -coordinate position of the selected primary vertex with respect to the true Higgs boson production vertex. The signal shape for these events is modeled by a sum of between one and four (two and three) Gaussian functions in the case of the 8 (13) TeV data, depending on the event class. In both cases, the means, widths, and relative fractions of the Gaussian functions are determined by the fits.

The full signal model for all values of m_H is obtained by linear interpolation of each of the fitted parameters. The final parameterized shapes for the combination of all production mechanisms, for all event classes, weighted by their SM cross sections are shown in Fig. 1 for a Higgs boson mass of 90 GeV for the 8 and 13 TeV data. Also shown are the full width at half maximum (FWHM) value and the value of the effective standard deviation for signal (σ_{eff}), which is defined as half the width of the narrowest interval containing 68.3% of the invariant mass distribution. The product of efficiency and acceptance of the signal model ranges from 36.2 (22.7)% for $m_H = 80$ (70) GeV to 40.4 (26.5)% for $m_H = 110$ (110) GeV in the case of the 8 (13) TeV data.

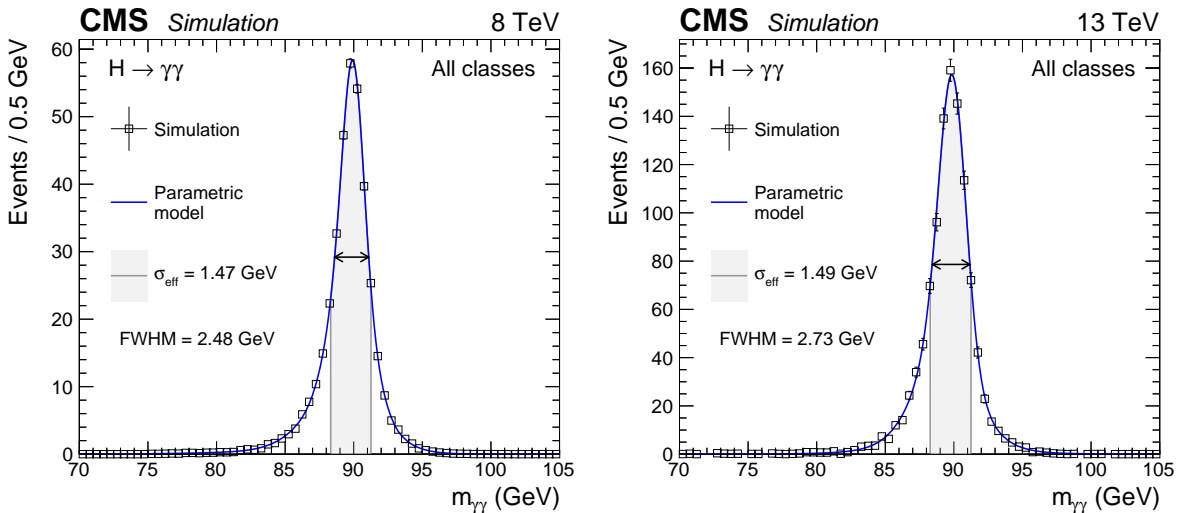


Figure 1: Full parameterized signal shape, integrated over all event classes, in simulated signal events with $m_H = 90$ GeV at $\sqrt{s} = 8$ TeV (left) and 13 TeV (right). The open points are the weighted MC events and the blue lines the corresponding parametric models. Also shown are the σ_{eff} values and the shaded region limited by $\pm\sigma_{\text{eff}}$, along with the FWHM values, indicated by the position of the arrows on each distribution.

5 Background estimation

In this analysis, as in [11, 40, 41], the background is modeled by fitting analytic functions to the observed diphoton mass distributions, in each of the event classes. The fits are performed over the range $75 (65) < m_{\gamma\gamma} < 120$ GeV for the 8 (13) TeV data. In the case of the 8 TeV data, a single fit function is chosen for each class after a study of the potential bias in the estimated background, which is required to be negligible, following the method used in [11]. For the 13 TeV data, as in [40, 41], the model is determined from data with the discrete profiling method [66], which treats the choice of the background function as a discrete parameter in the likelihood fit to the data and estimates the systematic uncertainty associated with the choice of a particular function.

Since the search mass range of this analysis includes the Z boson peak region, a significant potential background source is Drell–Yan dielectron production that, through misidentification, could appear to result in two isolated photons. Therefore, an explicit component intended to describe the background from the Drell–Yan process in which the two apparent isolated photons survive all the selection requirements as stated in Section 3.2, is added to the smoothly falling polynomial distribution used to model the background in [11, 40, 41]. This additional component, referred to as “doubly misidentified” events, is modeled with a double-sided Crystal Ball (DCB) function, which is a modification of the Crystal Ball function [67] with an exponential tail on both sides. The DCB function is characterized by seven parameters: the number of events for normalization, the Gaussian mean and standard deviation, and the four additional shape parameters α_L , n_L , α_R , and n_R , where $\alpha_{L,R}$ and $n_{L,R}$ refer, respectively, to the slope and normalization of the left-hand (L) and right-hand (R) exponential tails. The values of the DCB shape parameters are determined by fitting the diphoton invariant mass distribution in a sample of simulated Drell–Yan doubly misidentified events for each event class. Because of the small size of the simulated event sample, we fix two of the six DCB shape parameters, α_L and α_R , to make the fit more stable. The fixed values are different in each event class and are obtained using the normalized χ^2 value for the 8 TeV data, and the minimal maximum pull value for the 13 TeV data, as a figure of merit. In each class the value of the mean, which coincides with the peak position, lies somewhat below the nominal Z boson mass value. This is due to the fact that the electrons surviving the photon selection requirements (in particular the electron veto) have in general been poorly reconstructed, for example having undergone wide-angle bremsstrahlung of high-energy photons; furthermore, the electron energies have been corrected with factors developed for photons.

For both the choice of the single fit function in the case of the 8 TeV data, and the application of the discrete profiling method in the case of the 13 TeV data, members of several families of analytic functions, including exponential, power law, Bernstein, and Laurent series are considered, each summed with a DCB function. The maximum order term in each series is determined using an F-test [68]. In the analysis of the 13 TeV data, the minimum order of the series is determined as well, using a goodness-of-fit test.

In the analysis of the 8 TeV data these functions, called “truth models”, are used to generate MC pseudo-data sets that are fitted with candidate functions from the same families of an order within the range determined by the above tests. The bias for a given candidate function to fit a given truth model is defined as the average pull of the fitted signal strength modifier over the set of relevant generated pseudo-data sets, and is required to be less than 0.14 to be considered negligible. This amount of bias necessitates an increase in the uncertainty in the frequentist coverage of the signal strength of less than 1%, which is deemed acceptable. The final background function is chosen from the candidate functions that fit all truth models in a

given event class with negligible bias.

In the discrete profiling method used for the analysis of the 13 TeV data, when fitting these functions to the background $m_{\gamma\gamma}$ distribution, the value of twice the negative logarithm of the likelihood (2NLL) is minimized. A penalty is added to the 2NLL value to take into account the number of floating parameters, including the fraction of background events attributed to the component arising from the doubly misidentified events (DCB fraction), in each candidate function.

In both methods, the normalization of the Drell–Yan background is determined in the fit. The shape parameters are constrained to the constant values that are obtained by fitting the doubly misidentified Drell–Yan events, as described above. In particular, the value of the Gaussian standard deviation in each event class is greater than the corresponding value of σ_{eff} in the signal model by a factor of up to 2.

For the analysis of the 8 TeV data, the sum of a fifth-order Bernstein polynomial and the DCB function is chosen as the final background model for event classes 1, 2, and 3. For class 0, a fourth-order Bernstein polynomial is used. For the 13 TeV data, a third-order exponential series plus the DCB function is chosen for classes 0 and 2, and a first-order power-law series plus the DCB function for class 1. The DCB fractions for these chosen models in the subset of the diphoton mass range extending from 85 to 95 GeV, the most relevant for dielectron background from the Drell–Yan process, are, for the 8 (13) TeV data, 3.0, 5.6, 2.6, and 5.1 (3.0, 3.1, and 3.3)%, respectively, for event classes 0, 1, 2, and 3 (0, 1, and 2).

Binned likelihood fits of the chosen background models to the observed diphoton mass distribution, assuming no signal, are shown for all the event classes in Fig. 2 (3) for the 8 (13) TeV data. The one- and two-standard deviation (σ) bands include only the uncertainty in the background model normalization associated with the statistical uncertainties of the fits, and are thus shown for illustration purposes only. They are obtained using an extended likelihood fit parametrized in terms of the background yield in a window that is the size of the bin widths in Figs. 2 and 3. The corresponding signal model for $m_H = 90$ GeV, multiplied by 10, is also shown for illustration purposes.

6 Systematic uncertainties

Many of the systematic uncertainties relevant to the analyses performed in [11, 40, 41] also apply to this analysis and are described briefly below. Additional uncertainties specific to this analysis are described in more detail.

6.1 Uncertainties evaluated at the per-photon level

The systematic uncertainties in the shape of the photon identification BDT distribution and in the per-photon energy resolution described in [40, 41] are applied in this analysis. These uncertainties propagate to the multivariate event classifier value, giving rise to the migration of events from one class to another, and to variations in the per-event efficiency in each class and for each production process. The uncertainties are evaluated using a signal sample with $m_H = 105$ (90) GeV for the analysis of the 8 (13) TeV data. For the 8 TeV data, the largest variation in efficiency due to the photon identification BDT distribution shape is 5.9%, for the VBF process in event class 3. For the 13 TeV data the largest variation is 14.6% for the VBF process in event class 2, with other processes in class 2 having variations of less than 11%, and variations in the other classes being below 5%. The largest variation in the efficiency due to the per-photon energy resolution applicable to the 8 TeV data is 13.7% for the ggH process in class 0; otherwise

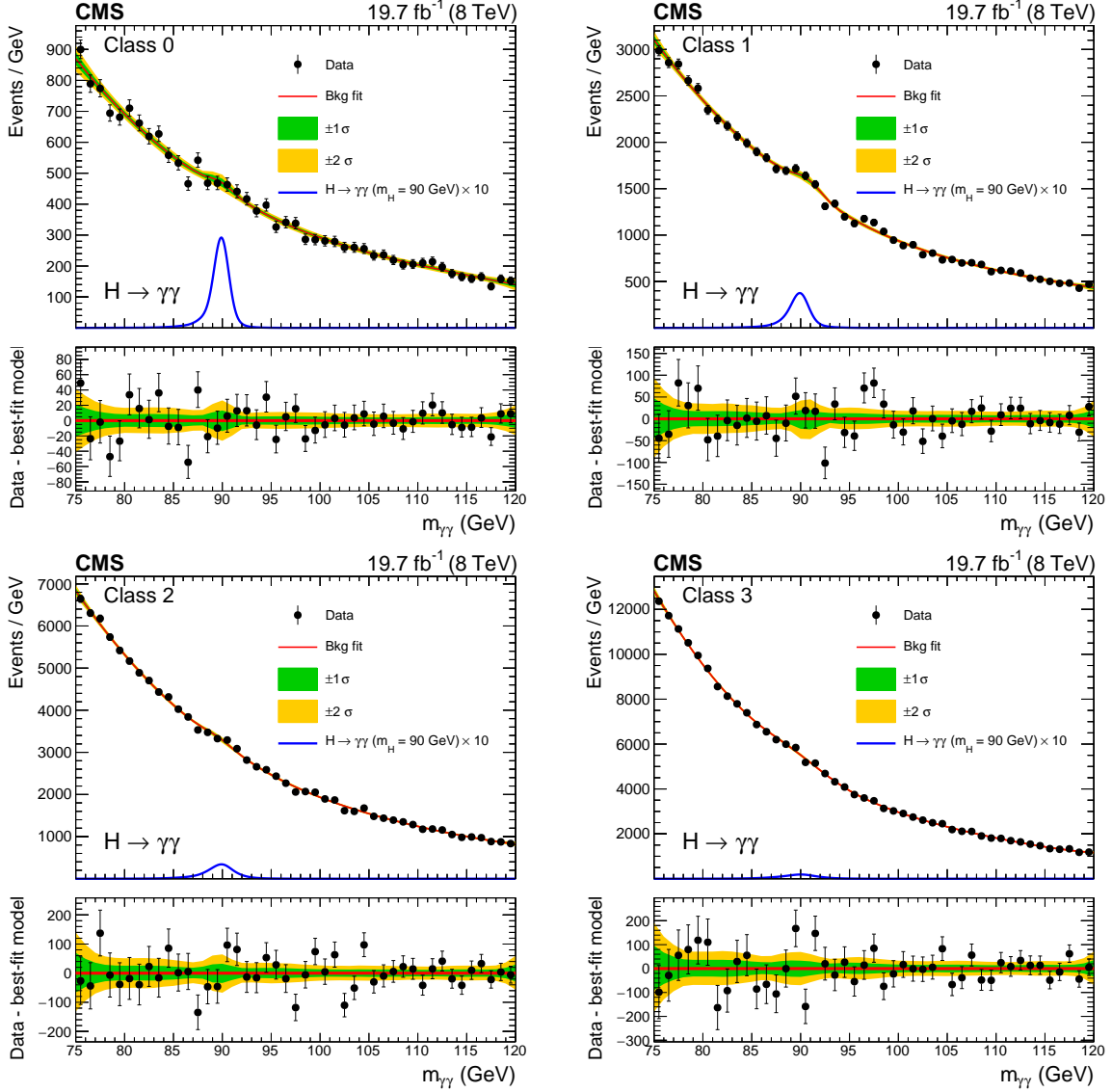


Figure 2: Background model fits using the chosen “best-fit” parametrization to data in the four event classes at $\sqrt{s} = 8$ TeV. The corresponding signal model for each class for $m_H = 90$ GeV, multiplied by 10, is also shown. The one- and two- σ bands reflect the uncertainty in the background model normalization associated with the statistical uncertainties of the fits, and are shown for illustration purposes only. The difference between the data and the best-fit model is shown in the lower panels.

the variations are below 9%. For the 13 TeV data, the largest variation is 7% for the VBF process in class 2; otherwise the variations are below 5%.

For the 8 (13) TeV data, uncertainties in the trigger efficiencies give rise to efficiency variations of 1 (less than 1)%, and in the scale factors of the preselection, of less than 1.5 (5.5)%. In the case of the 13 TeV data, the uncertainties in the scale factors of the electron veto and of the minimum value of the photon identification BDT are considered as supplemental sources of efficiency variations, which amount to less than 2% for each.

The uncertainties in the measurement and in the correction of the photon energy scale in data, and in the correction of the energy resolution in simulation, arising from the methodology ex-

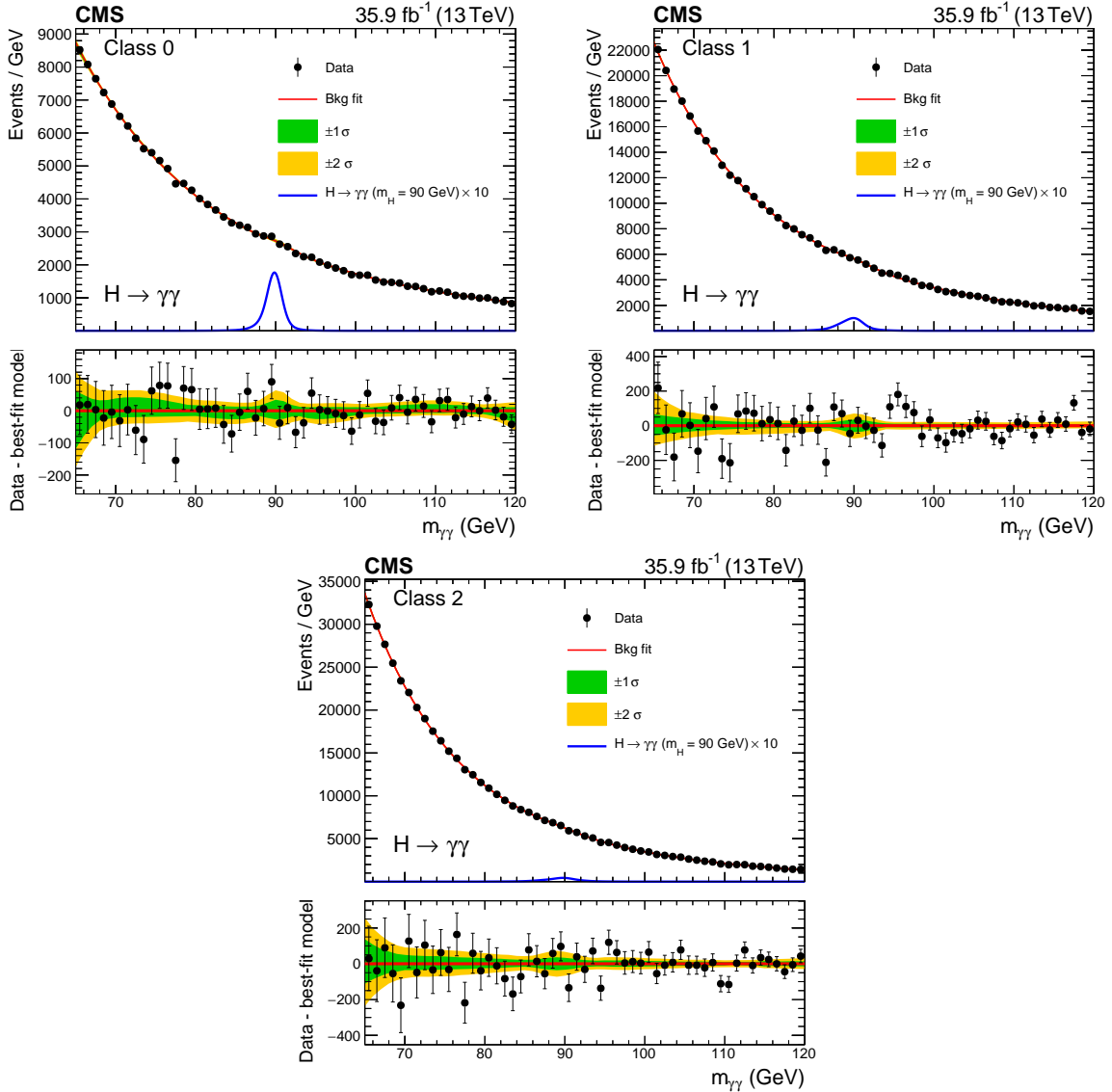


Figure 3: Background model fits using the chosen “best-fit” parametrization to data in the three event classes at $\sqrt{s} = 13$ TeV. The corresponding signal model for each class for $m_H = 90$ GeV, multiplied by 10, is also shown. The one- and two- σ bands reflect the uncertainty in the background model normalization associated with the statistical uncertainties of the fits, and are shown for illustration purposes only. The difference between the data and the best-fit model is shown in the lower panels.

plotting $Z \rightarrow e^+e^-$ events as described in Section 4 and [40, 41], are calculated in the same bins as the corrections themselves. Uncertainties arising from modeling of the material budget and of nonuniformity of light collection (the fraction of crystal scintillation light detected as a function of its longitudinal depth when emitted), nonlinearity in the photon energy scale between data and simulation, imperfect electromagnetic shower simulation, and vertex finding [40, 41], are propagated to the parametric signal model, where they result in uncertainties in the diphoton efficiency, mass scale, and resolution.

6.2 Uncertainties evaluated at the per-event level

The per-event systematic uncertainty in the total integrated luminosity, estimated from data [69, 70], contributes an uncertainty of 2.6 (2.5)% in the signal yield for the 8 (13) TeV data.

The systematic uncertainties from the theoretical predictions considered in this analysis are of two types. Firstly, the uncertainties in the signal acceptance due to changes in particle p_T and η values, arising from variations in the PDF and renormalization and factorization scales, are calculated [40, 41] using a signal sample with $m_H = 105$ (90) GeV for the analysis of the 8 (13) TeV data. The CT10 [55] PDF set (NNPDF3.0 [56] PDF set using the MC2HESSIAN procedure [71]) is used to estimate the PDF variations in the case of the 8 (13) TeV data. In the case of the 13 TeV data, the effects due to variations of the strong coupling strength, α_S , are also considered, following the PDF4LHC prescription [60, 72]. The uncertainty of greatest magnitude due to PDF variations, in the 8 TeV data, is 2% for the VBF production process in event class 0; otherwise the uncertainties are below 1% and, in many cases, well below 1%. In the 13 TeV data, the uncertainties are equal to or less than 0.4%. The largest uncertainty due to scale variations, in the 8 TeV data, is 7.5% for the ggH production process in event class 0; otherwise the uncertainties are below 1%. In the 13 TeV data, the largest uncertainties also occur for the ggH process, with the maximum of 3.8% again occurring in event class 0. The uncertainties due to variations in α_S , considered for the 13 TeV data, are typically below 0.5%, with the largest uncertainty of 0.7% occurring for the VBF process in event class 2.

Secondly, the uncertainties in the production cross sections for an SM-like Higgs boson, at center-of-mass energies of 8 and 13 TeV, are accounted for following the recommendations of the LHC Higgs cross section working group [60]. These uncertainties are due to PDF, α_S , and scale variations. They are used in the calculation of the expected and observed limits on the product of the production cross section and branching fraction into two photons relative to the expected value for an SM-like Higgs boson, and in the calculations of the expected and observed local p -values. The uncertainty in the branching fraction into two photons is neglected.

An additional source of per-event systematic uncertainty specific to this analysis is the modeling of the Z boson resonance component of the background. As explained previously, the parameters of the DCB function used to model the Z boson resonance are obtained from doubly misidentified events, which are simulated Drell–Yan events with all selection requirements applied including the electron veto requirement. These parameters could be different for data and simulation. To estimate these differences, we study simulated events from the Drell–Yan, diphoton, $\gamma + \text{jet}$, and QCD physics processes where one photon candidate survives all selection requirements including the electron veto, and the other survives all selection requirements but fails the electron veto (“singly misidentified” events). We fit the invariant diphoton mass of these events in data, in simulation including the sum of all background processes, and in simulated Drell–Yan events alone, with a DCB plus an exponential component that describes the additional continuum background inherent in singly misidentified events. We consider the pairwise differences among the DCB mean and standard deviation parameters extracted from these three types of fits for each event class. The differences are considered statistically significant if greater than the quadratic sum of the statistical uncertainties from the fit. These differences will contribute to the total systematic uncertainty in the DCB parameter values. The nominal parameter values are obtained from doubly misidentified events so the differences contributing to the parameter uncertainties that are estimated from singly misidentified events are doubled, to reflect the more conservative case where the parameters of the two photon candidates in a doubly misidentified event are completely correlated.

The total systematic uncertainty in each event class for the mean and standard deviation pa-

Table 1: The expected number of SM-like Higgs boson signal events ($m_H = 90$ GeV) per event class and the corresponding percentage breakdown per production process, for the 8 and 13 TeV data. The values of σ_{eff} and σ_{HM} are also shown, along with the number of background events (“Bkg.”) per GeV estimated from the background-only fit to the data, that includes the number, shown separately, from the Drell–Yan process (“DY Bkg.”), in a σ_{eff} window centered on $m_H = 90$ GeV.

Event classes		Expected SM-like Higgs boson signal yield ($m_H = 90$ GeV)							σ_{eff} (GeV)	σ_{HM} (GeV)	Bkg. (GeV ⁻¹)	DY Bkg. (GeV ⁻¹)
		Total	ggH (%)	VBF (%)	WH (%)	ZH (%)	$t\bar{t}H$ (%)					
8 TeV	0	64	68.9	14.9	8.8	4.8	2.5	0.94	0.78	467	30	
19.7 fb ⁻¹	1	100	87.5	5.3	4.3	2.3	0.7	1.20	0.96	1639	157	
	2	121	90.0	3.9	3.7	2.0	0.5	1.61	1.26	3278	145	
	3	89	92.2	2.8	3.0	1.6	0.3	2.11	1.68	5508	383	
	Total	374	86.2	5.9	4.6	2.4	0.8	1.47	1.05	10 892	715	
13 TeV	0	457	80.2	9.7	4.9	2.8	2.5	1.11	0.96	2720	132	
35.9 fb ⁻¹	1	395	90.1	4.1	3.2	1.7	0.9	1.69	1.45	5636	282	
	2	214	92.0	3.3	2.6	1.4	0.7	2.18	1.73	6256	274	
	Total	1066	86.2	6.3	3.8	2.1	1.6	1.49	1.16	14 612	688	

rameters, is then the quadratic sum of: the statistical uncertainty from the fit to the doubly misidentified simulated Drell–Yan events; the doubled difference between the parameter values from data and from the sum of all simulated background processes; and the doubled difference between the parameter values from the sum of all simulated background processes and from simulated Drell–Yan events alone, determined from the singly misidentified events. As a conservative measure in the case of the 8 TeV data, the doubled differences in the parameter values for the event class where the values are maximal are used for all four classes.

Finally, the analysis takes into account the statistical uncertainties in the values of the DCB n_L and n_R parameters obtained from the fits to the doubly misidentified simulated $Z \rightarrow e^+e^-$ events.

7 Results

Table 1 shows the expected number of signal events corresponding to the production of a hypothetical additional SM-like Higgs boson with $m_H = 90$ GeV, from the analyses of the 8 and 13 TeV data. The total number is broken down into the contributions from all the production processes in each of the event classes, where the VH processes corresponding to W and Z are listed separately. Also shown are the σ_{eff} and σ_{HM} (defined as the FWHM divided by 2.35) values, as well as the number of background events per GeV estimated from the background-only fit to the data, that includes the number, shown separately, from the Drell–Yan process, in the corresponding σ_{eff} window centered on $m_H = 90$ GeV, using the chosen background function.

A simultaneous binned maximum likelihood fit to the diphoton invariant mass distributions in all event classes, with a step size of 0.1 GeV, is performed over the range $75 (65) < m_{\gamma\gamma} < 120$ GeV for the 8 (13) TeV data, using an asymptotic approach [73–75] with a test statistic based on the profile likelihood ratio [76]. The expected and observed 95% confidence level (CL) upper limits on the product of the cross section (σ_H) and branching fraction (\mathcal{B}) into two photons for an additional SM-like Higgs boson, from the analysis of each of the 8 and 13 TeV data sets, are presented in Fig. 4 for the parametric signal model. No significant ($>3\sigma$) excess with respect to the expected number of background events is observed. For the 8 TeV data, the minimum (max-

imum) observed upper limit on the product of the production cross section and branching fraction is approximately 31 (129) fb, corresponding to a mass hypothesis of 102.8 (91.0) GeV. For the 13 TeV data, the minimum (maximum) observed upper limits are 26 (161) fb, corresponding to a mass hypothesis of 103.0 (89.8) GeV.

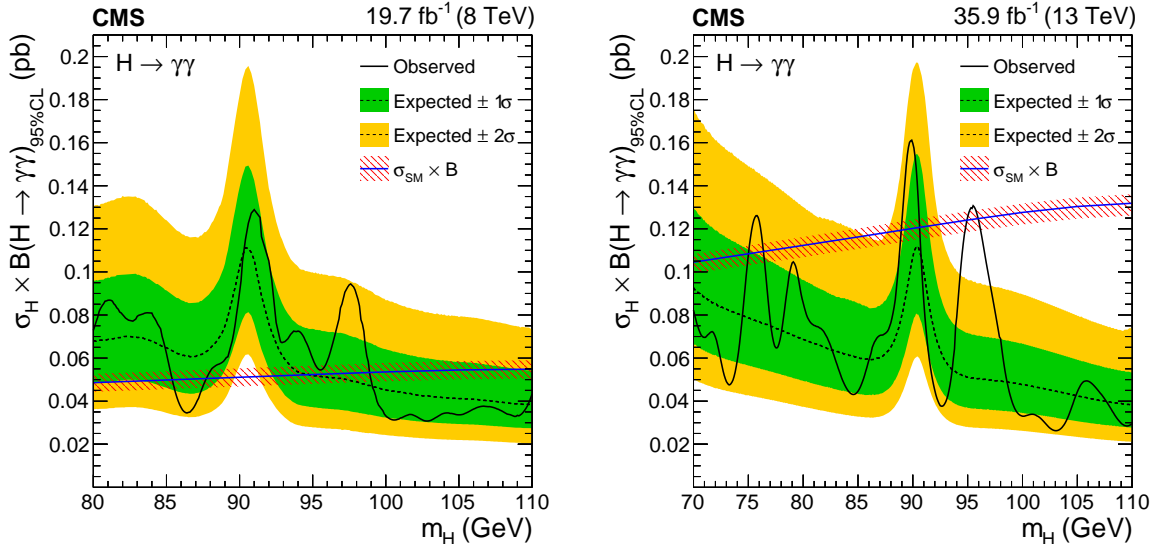


Figure 4: Expected and observed exclusion limits (95% CL, in the asymptotic approximation) on the product of the production cross section and branching fraction into two photons for an additional SM-like Higgs boson, from the analysis of the 8 (left) and 13 (right) TeV data. The inner and outer bands indicate the regions containing the distribution of limits located within ± 1 and 2σ , respectively, of the expectation under the background-only hypothesis. The corresponding theoretical prediction for the product of the cross section and branching fraction into two photons for an additional SM-like Higgs boson is shown as a solid line with a hatched band, indicating its uncertainty [60].

In addition, the expected and observed 95% CL upper limits for the ggH plus $t\bar{t}H$ processes and for the VBF plus VH processes are shown in Fig. 5 for each of the 8 and 13 TeV data sets. The production processes, in each case, are combined assuming relative proportions as predicted by the SM.

The results from the 8 and 13 TeV data are combined statistically applying the same methods used to obtain the results from each individual data set, in the diphoton invariant mass range common to the two data sets, $80 < m_{\gamma\gamma} < 110$ GeV. All of the experimental systematic uncertainties as well as the theoretical uncertainties in the signal acceptance due to PDF variations are assumed to be uncorrelated between the two data sets. The theoretical uncertainties in the signal acceptance due to scale variations as well as in the production cross sections at the center-of-mass energies of 8 and 13 TeV for an additional SM-like Higgs boson are assumed to be fully correlated. Figure 6 shows the expected and observed 95% CL upper limits on the product of the cross section and branching fraction into two photons for an additional Higgs boson, relative to the SM-like value from the latest theoretical predictions from the LHC Higgs cross section working group [60]. No significant excess with respect to the expected number of background events is observed. The minimum (maximum) observed upper limit on the product of the production cross section and branching fraction normalized to the SM-like value is 0.17 (1.13) corresponding to a mass hypothesis of 103.0 (90.0) GeV. Figure 7 shows the expected and observed local p -values as a function of the mass of an additional SM-like Higgs boson, calculated with respect to the background-only hypothesis, from the analyses of the 8

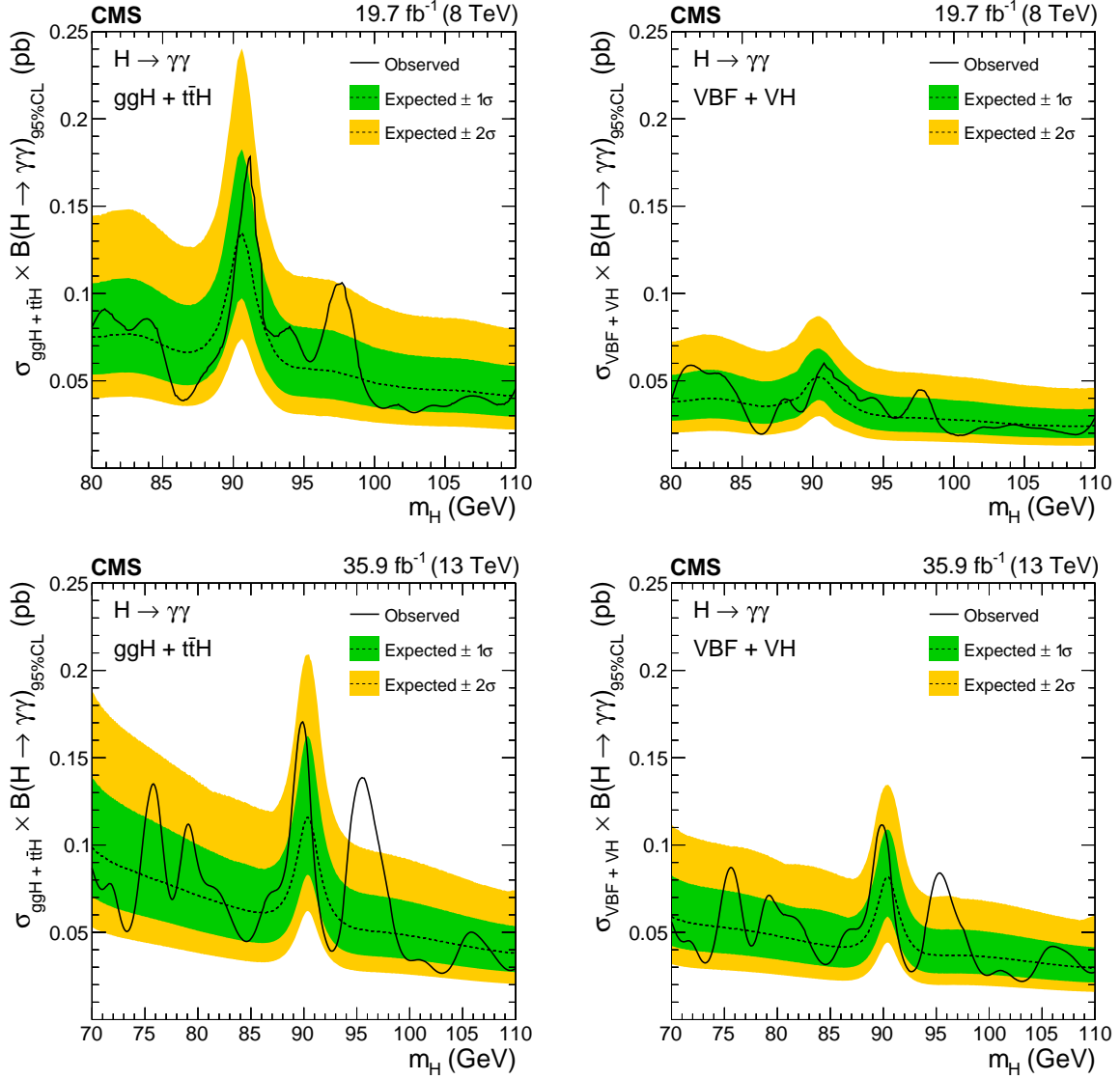


Figure 5: Expected and observed exclusion limits (95% CL, in the asymptotic approximation) on the product of the production cross section and branching fraction into two photons for an additional SM-like Higgs boson, for the ggH plus $t\bar{t}H$ (left) and VBF plus VH (right) processes, from the analysis of the 8 (top) and 13 (bottom) TeV data. The inner and outer bands indicate the regions containing the distribution of limits located within ± 1 and 2σ , respectively, of the expectation under the background-only hypothesis.

and 13 TeV data, and from their combination. The most significant expected sensitivity occurs at the highest explored mass hypothesis of 110 GeV with a local expected significance close to 3σ ($>6\sigma$) for the 8 (13) TeV data, while the worst expected significance occurs in the neighborhood of 90 GeV, where it is approximately 0.4σ (slightly above 2σ). For the combination, the most (least) significant expected sensitivity occurs at a mass hypothesis of 110 (90) GeV with a local expected significance of approximately 6.8σ (slightly above 2.0σ). In the case of the 8 TeV data, one excess with approximately 2.0σ local significance is observed for a mass hypothesis of 97.7 GeV. For the 13 TeV data, one excess with approximately 2.90σ local (1.47σ global) significance is observed for a mass hypothesis of 95.3 GeV, where the global significance has been calculated using the method of [77]. In the combination, an excess with approximately 2.8σ

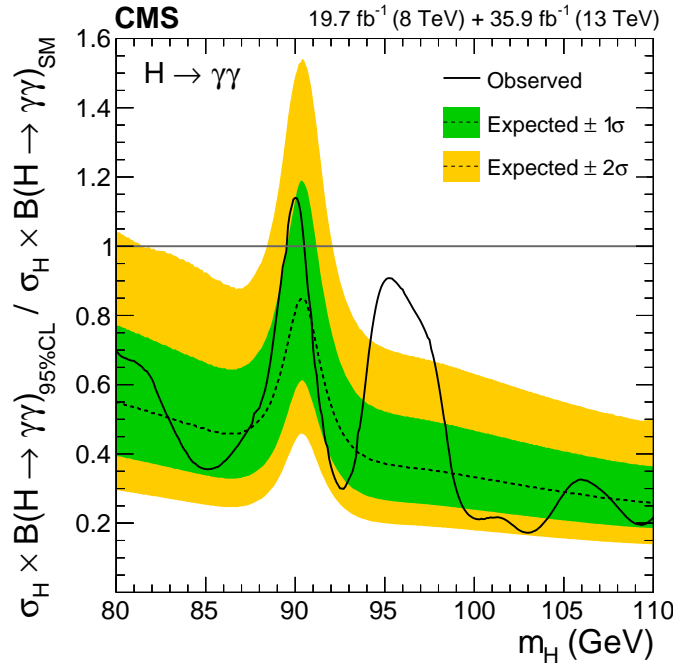


Figure 6: Expected and observed exclusion limits (95% CL, in the asymptotic approximation) on the product of the production cross section and branching fraction into two photons for an additional Higgs boson, relative to the expected SM-like value, from the analysis of the 8 and 13 TeV data. The inner and outer bands indicate the regions containing the distribution of limits located within ± 1 and 2σ , respectively, of the expectation under the background-only hypothesis.

local (1.3σ global) significance is observed for a mass hypothesis of 95.3 GeV.

8 Summary

A search for an additional, SM-like, low-mass Higgs boson decaying into two photons has been presented. It is based upon data samples corresponding to integrated luminosities of 19.7 and 35.9 fb^{-1} collected at center-of-mass energies of 8 TeV in 2012 and 13 TeV in 2016, respectively. The search is performed in a mass range between 70 and 110 GeV. The expected and observed 95% CL upper limits on the product of the production cross section and branching fraction into two photons for an additional SM-like Higgs boson as well as the expected and observed local p -values are presented. No significant ($>3\sigma$) excess with respect to the expected number of background events is observed. The observed upper limit on the product of the production cross section and branching fraction for the 2012 (2016) data set ranges from 129 (161) fb to 31 (26) fb. The statistical combination of the results from the analyses of the two data sets in the common mass range between 80 and 110 GeV yields an upper limit on the product of the cross section and branching fraction, normalized to that for a standard model-like Higgs boson, ranging from 0.7 to 0.2, with two notable exceptions: one in the region around the Z boson peak, where the limit rises to 1.1, which may be due to the presence of Drell–Yan dielectron production where electrons could be misidentified as isolated photons, and a second due to an observed excess with respect to the standard model prediction, which is maximal for a mass hypothesis of 95.3 GeV with a local (global) significance of 2.8 (1.3) standard deviations. More data are required to ascertain the origin of this excess. This is the first search for new resonances

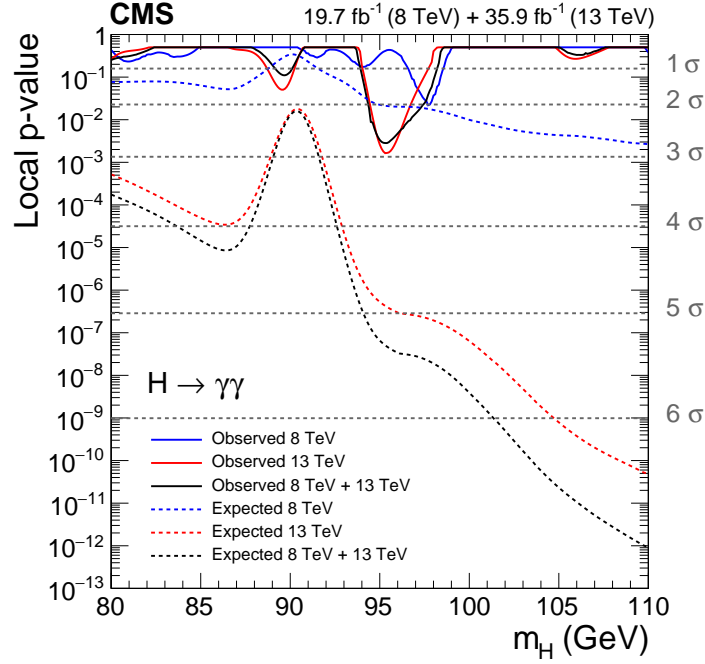


Figure 7: Expected and observed local p -values as a function of m_H for the 8 and 13 TeV data and their combination (solid curves) plotted together with the relevant expectations for an additional SM-like Higgs boson (dotted curves).

in the diphoton final state in this mass range based on LHC data at a center-of-mass energy of 13 TeV.

Acknowledgments

We congratulate our colleagues in the CERN accelerator departments for the excellent performance of the LHC and thank the technical and administrative staffs at CERN and at other CMS institutes for their contributions to the success of the CMS effort. In addition, we gratefully acknowledge the computing centers and personnel of the Worldwide LHC Computing Grid for delivering so effectively the computing infrastructure essential to our analyses. Finally, we acknowledge the enduring support for the construction and operation of the LHC and the CMS detector provided by the following funding agencies: BMBWF and FWF (Austria); FNRS and FWO (Belgium); CNPq, CAPES, FAPERJ, FAPERGS, and FAPESP (Brazil); MES (Bulgaria); CERN; CAS, MoST, and NSFC (China); COLCIENCIAS (Colombia); MSES and CSF (Croatia); RPF (Cyprus); SENESCYT (Ecuador); MoER, ERC IUT, and ERDF (Estonia); Academy of Finland, MEC, and HIP (Finland); CEA and CNRS/IN2P3 (France); BMBF, DFG, and HGF (Germany); GSRT (Greece); NKFI (Hungary); DAE and DST (India); IPM (Iran); SFI (Ireland); INFN (Italy); MSIP and NRF (Republic of Korea); MES (Latvia); LAS (Lithuania); MOE and UM (Malaysia); BUAP, CINVESTAV, CONACYT, LNS, SEP, and UASLP-FAI (Mexico); MOS (Montenegro); MBIE (New Zealand); PAEC (Pakistan); MSHE and NSC (Poland); FCT (Portugal); JINR (Dubna); MON, RosAtom, RAS, RFBR, and NRC KI (Russia); MESTD (Serbia); SEIDI, CPAN, PCTI, and FEDER (Spain); MOSTR (Sri Lanka); Swiss Funding Agencies (Switzerland); MST (Taipei); ThEPCenter, IPST, STAR, and NSTDA (Thailand); TUBITAK and TAEK (Turkey); NASU and SFFR (Ukraine); STFC (United Kingdom); DOE and NSF (USA).

Individuals have received support from the Indo-French Network in High Energy Physics fi-

nanced by the Indo-French Center for the Promotion of Advanced Research (CEFIPRA/IFCPAR), the Marie-Curie program and the European Research Council and Horizon 2020 Grant, contract No. 675440 (European Union); the Leventis Foundation; the A. P. Sloan Foundation; the Alexander von Humboldt Foundation; the Belgian Federal Science Policy Office; the Fonds pour la Formation à la Recherche dans l'Industrie et dans l'Agriculture (FRIA-Belgium); the Agentschap voor Innovatie door Wetenschap en Technologie (IWT-Belgium); the F.R.S.-FNRS and FWO (Belgium) under the "Excellence of Science - EOS" - be.h project n. 30820817; the Ministry of Education, Youth and Sports (MEYS) of the Czech Republic; the Lendület ("Momentum") Program and the János Bolyai Research Scholarship of the Hungarian Academy of Sciences, the New National Excellence Program ÚNKP, the NKFIÁ research grants 123842, 123959, 124845, 124850 and 125105 (Hungary); the Council of Science and Industrial Research, India; the HOMING PLUS program of the Foundation for Polish Science, cofinanced from European Union, Regional Development Fund, the Mobility Plus program of the Ministry of Science and Higher Education, the National Science Center (Poland), contracts Harmonia 2014/14/M/ST2/00428, Opus 2014/13/B/ST2/02543, 2014/15/B/ST2/03998, and 2015/19/B/ST2/02861, Sonata-bis 2012/07/E/ST2/01406; the National Priorities Research Program by Qatar National Research Fund; the Programa Estatal de Fomento de la Investigación Científica y Técnica de Excelencia María de Maeztu, grant MDM-2015-0509 and the Programa Severo Ochoa del Principado de Asturias; the Thalís and Aristeia programs cofinanced by EU-ESF and the Greek NSRF; the Rachadapisek Sompot Fund for Postdoctoral Fellowship, Chulalongkorn University and the Chulalongkorn Academic into Its 2nd Century Project Advancement Project (Thailand); the Welch Foundation, contract C-1845; and the Weston Havens Foundation (USA).

References

- [1] S. L. Glashow, "Partial-symmetries of weak interactions", *Nucl. Phys.* **22** (1961) 579, doi:10.1016/0029-5582(61)90469-2.
- [2] S. Weinberg, "A model of leptons", *Phys. Rev. Lett.* **19** (1967) 1264, doi:10.1103/PhysRevLett.19.1264.
- [3] A. Salam, "Weak and electromagnetic interactions", in *Elementary particle physics: relativistic groups and analyticity*, N. Svartholm, ed., p. 367. Almqvist & Wiksell, Stockholm, 1968. Proceedings of the eighth Nobel symposium.
- [4] F. Englert and R. Brout, "Broken symmetry and the mass of gauge vector mesons", *Phys. Rev. Lett.* **13** (1964) 321, doi:10.1103/PhysRevLett.13.321.
- [5] P. W. Higgs, "Broken symmetries, massless particles and gauge fields", *Phys. Lett.* **12** (1964) 132, doi:10.1016/0031-9163(64)91136-9.
- [6] P. W. Higgs, "Broken symmetries and the masses of gauge bosons", *Phys. Rev. Lett.* **13** (1964) 508, doi:10.1103/PhysRevLett.13.508.
- [7] G. S. Guralnik, C. R. Hagen, and T. W. B. Kibble, "Global conservation laws and massless particles", *Phys. Rev. Lett.* **13** (1964) 585, doi:10.1103/PhysRevLett.13.585.
- [8] P. W. Higgs, "Spontaneous symmetry breakdown without massless bosons", *Phys. Rev.* **145** (1966) 1156, doi:10.1103/PhysRev.145.1156.

-
- [9] T. W. B. Kibble, "Symmetry breaking in non-Abelian gauge theories", *Phys. Rev.* **155** (1967) 1554, doi:10.1103/PhysRev.155.1554.
- [10] ATLAS Collaboration, "Observation of a new particle in the search for the standard model Higgs boson with the ATLAS detector at the LHC", *Phys. Lett. B* **716** (2012) 1, doi:10.1016/j.physletb.2012.08.020, arXiv:1207.7214.
- [11] CMS Collaboration, "Observation of a new boson at a mass of 125 GeV with the CMS experiment at the LHC", *Phys. Lett. B* **716** (2012) 30, doi:10.1016/j.physletb.2012.08.021, arXiv:1207.7235.
- [12] CMS Collaboration, "Observation of a new boson with mass near 125 GeV in pp collisions at $\sqrt{s} = 7$ and 8 TeV", *JHEP* **06** (2013) 081, doi:10.1007/JHEP06(2013)081, arXiv:1303.4571.
- [13] A. Celis, V. Ilisie, and A. Pich, "LHC constraints on two-Higgs doublet models", *JHEP* **07** (2013) 053, doi:10.1007/JHEP07(2013)053, arXiv:1302.4022.
- [14] B. Coleppa, F. Kling, and S. Su, "Constraining type II 2HDM in light of LHC Higgs searches", *JHEP* **01** (2014) 161, doi:10.1007/JHEP01(2014)161, arXiv:1305.0002.
- [15] S. Chang et al., "Two Higgs doublet models for the LHC Higgs boson data at $\sqrt{s} = 7$ and 8 TeV", *JHEP* **09** (2014) 101, doi:10.1007/JHEP09(2014)101, arXiv:1310.3374.
- [16] J. Bernon et al., "Scrutinizing the alignment limit in two-Higgs-doublet models. II. $m_h=125$ GeV", *Phys. Rev. D* **93** (2016) 035027, doi:10.1103/PhysRevD.93.035027, arXiv:1511.03682.
- [17] G. Cacciapaglia et al., "Search for a lighter Higgs boson in two Higgs doublet models", *JHEP* **12** (2016) 68, doi:10.1007/JHEP12(2016)068, arXiv:1607.08653.
- [18] P. Fayet, "Supergauge invariant extension of the Higgs mechanism and a model for the electron and its neutrino", *Nucl. Phys. B* **90** (1975) 104, doi:10.1016/0550-3213(75)90636-7.
- [19] R. Barbieri, S. Ferrara, and C. A. Savoy, "Gauge models with spontaneously broken local supersymmetry", *Phys. Lett. B* **119** (1982) 343, doi:10.1016/0370-2693(82)90685-2.
- [20] M. Dine, W. Fischler, and M. Srednicki, "A simple solution to the strong CP problem with a harmless axion", *Phys. Lett. B* **104** (1981) 199, doi:10.1016/0370-2693(81)90590-6.
- [21] H. P. Nilles, M. Srednicki, and D. Wyler, "Weak interaction breakdown induced by supergravity", *Phys. Lett. B* **120** (1983) 346, doi:10.1016/0370-2693(83)90460-4.
- [22] J. M. Frère, D. R. T. Jones, and S. Raby, "Fermion masses and induction of the weak scale by supergravity", *Nucl. Phys. B* **222** (1983) 11, doi:10.1016/0550-3213(83)90606-5.
- [23] J. P. Derendinger and C. A. Savoy, "Quantum effects and $SU(2) \times U(1)$ breaking in supergravity gauge theories", *Nucl. Phys. B* **237** (1984) 307, doi:10.1016/0550-3213(84)90162-7.

- [24] J. Ellis et al., “Higgs bosons in a nonminimal supersymmetric model”, *Phys. Rev. D* **39** (1989) 844, doi:10.1103/PhysRevD.39.844.
- [25] M. Drees, “Supersymmetric models with extended Higgs sector”, *Int. J. Mod. Phys. A* **4** (1989) 3635, doi:10.1142/S0217751X89001448.
- [26] U. Ellwanger, M. Rausch de Traubenberg, and C. A. Savoy, “Particle spectrum in supersymmetric models with a gauge singlet”, *Phys. Lett. B* **315** (1993) 331, doi:10.1016/0370-2693(93)91621-S, arXiv:hep-ph/9307322.
- [27] U. Ellwanger, M. Rausch de Traubenberg, and C. A. Savoy, “Higgs phenomenology of the supersymmetric model with a gauge singlet”, *Z. Phys. C* **67** (1995) 665, doi:10.1007/BF01553993, arXiv:hep-ph/9502206.
- [28] U. Ellwanger, M. Rausch de Traubenberg, and C. A. Savoy, “Phenomenology of supersymmetric models with a singlet”, *Nucl. Phys. B* **492** (1997) 21, doi:10.1016/S0550-3213(97)00128-4, arXiv:hep-ph/9611251.
- [29] T. Elliott, S. F. King, and P. L. White, “Unification constraints in the next-to-minimal supersymmetric standard model”, *Phys. Lett. B* **351** (1995) 213, doi:10.1016/0370-2693(95)00381-T, arXiv:hep-ph/9406303.
- [30] S. F. King and P. L. White, “Resolving the constrained minimal and next-to-minimal supersymmetric standard models”, *Phys. Rev. D* **52** (1995) 4183, doi:10.1103/PhysRevD.52.4183, arXiv:hep-ph/9505326.
- [31] F. Franke, “Neutralinos and Higgs bosons in the next-to-minimal supersymmetric standard model”, *Int. J. Mod. Phys. A* **12** (1997) 479, doi:10.1142/S0217751X97000529, arXiv:hep-ph/9512366.
- [32] M. Maniatis, “The next-to-minimal supersymmetric extension of the standard model reviewed”, *Int. J. Mod. Phys. A* **25** (2010) 3505, doi:10.1142/S0217751X10049827, arXiv:0906.0777.
- [33] U. Ellwanger, C. Hugonie, and A. M. Teixeira, “The next-to-minimal supersymmetric standard model”, *Phys. Rept.* **496** (2010) 1, doi:10.1016/j.physrep.2010.07.001, arXiv:0910.1785.
- [34] J.-W. Fan et al., “Study of diphoton decays of the lightest scalar Higgs boson in the next-to-minimal supersymmetric standard model”, *Chinese Physics C* **38** (2014) 073101, doi:10.1088/1674-1137/38/7/073101, arXiv:1309.6394.
- [35] U. Ellwanger and M. Rodriguez-Vazquez, “Discovery prospects of a light scalar in the NMSSM”, *JHEP* **02** (2016) 096, doi:10.1007/JHEP02(2016)096, arXiv:1512.04281.
- [36] M. Guchait and J. Kumar, “Diphoton signal of light pseudoscalar in NMSSM at the LHC”, *Phys. Rev. D* **95** (2017) 035036, doi:10.1103/PhysRevD.95.035036, arXiv:1608.05693.
- [37] J. Cao et al., “Diphoton signal of the light Higgs boson in natural NMSSM”, *Phys. Rev. D* **95** (2017) 116001, doi:10.1103/PhysRevD.95.116001, arXiv:1612.08522.

-
- [38] ALEPH Collaboration, DELPHI Collaboration, L3 Collaboration, OPAL Collaboration and the LEP working group for Higgs boson searches, “Search for the standard model Higgs boson at LEP”, *Phys. Lett. B* **565** (2003) 61, doi:10.1016/S0370-2693(03)00614-2, arXiv:hep-ex/0306033.
- [39] ATLAS Collaboration, “Search for scalar diphoton resonances in the mass range 65–600 GeV with the ATLAS detector in pp collision data at $\sqrt{s} = 8$ TeV”, *Phys. Rev. Lett.* **113** (2014) 171801, doi:10.1103/PhysRevLett.113.171801, arXiv:1407.6583.
- [40] CMS Collaboration, “Observation of the diphoton decay of the Higgs boson and measurement of its properties”, *Eur. Phys. J. C* **74** (2014) 3076, doi:10.1140/epjc/s10052-014-3076-z, arXiv:1407.0558.
- [41] CMS Collaboration, “Measurements of Higgs boson properties in the diphoton decay channel in proton-proton collisions at $\sqrt{s} = 13$ TeV”, *JHEP* **11** (2018) 185, doi:10.1007/JHEP11(2018)185, arXiv:1804.02716.
- [42] CMS Collaboration, “The CMS experiment at the CERN LHC”, *JINST* **3** (2008) S08004, doi:10.1088/1748-0221/3/08/S08004.
- [43] CMS Collaboration, “Performance of photon reconstruction and identification with the CMS detector in proton-proton collisions at $\sqrt{s} = 8$ TeV”, *JINST* **10** (2015) P08010, doi:10.1088/1748-0221/10/08/P08010, arXiv:1502.02702.
- [44] CMS Collaboration, “The CMS trigger system”, *JINST* **12** (2017) P01020, doi:10.1088/1748-0221/12/01/P01020, arXiv:1609.02366.
- [45] CMS Collaboration, “Measurement of the inclusive W and Z production cross sections in pp collisions at $\sqrt{s} = 7$ TeV”, *JHEP* **10** (2011) 132, doi:10.1007/JHEP10(2011)132, arXiv:1107.4789.
- [46] P. Nason, “A new method for combining NLO QCD with shower Monte Carlo algorithms”, *JHEP* **11** (2004) 040, doi:10.1088/1126-6708/2004/11/040, arXiv:hep-ph/0409146.
- [47] S. Frixione, P. Nason, and C. Oleari, “Matching NLO QCD computations with parton shower simulations: the POWHEG method”, *JHEP* **11** (2007) 070, doi:10.1088/1126-6708/2007/11/070, arXiv:0709.2092.
- [48] S. Alioli, P. Nason, C. Oleari, and E. Re, “A general framework for implementing NLO calculations in shower Monte Carlo programs: the POWHEG BOX”, *JHEP* **06** (2010) 043, doi:10.1007/JHEP06(2010)043, arXiv:1002.2581.
- [49] S. Alioli, P. Nason, C. Oleari, and E. Re, “NLO Higgs boson production via gluon fusion matched with shower in POWHEG”, *JHEP* **04** (2009) 002, doi:10.1088/1126-6708/2009/04/002, arXiv:0812.0578.
- [50] P. Nason and C. Oleari, “NLO Higgs boson production via vector-boson fusion matched with shower in POWHEG”, *JHEP* **02** (2010) 037, doi:10.1007/JHEP02(2010)037, arXiv:0911.5299.
- [51] T. Sjöstrand, S. Mrenna, and P. Skands, “PYTHIA 6.4 physics and manual”, *JHEP* **05** (2006) 026, doi:10.1088/1126-6708/2006/05/026, arXiv:hep-ph/0603175.

- [52] J. Alwall et al., “The automated computation of tree-level and next-to-leading order differential cross sections, and their matching to parton shower simulations”, *JHEP* **07** (2014) 079, doi:10.1007/JHEP07(2014)079, arXiv:1405.0301.
- [53] R. Frederix and S. Frixione, “Merging meets matching in MC@NLO”, *JHEP* **12** (2012) 061, doi:10.1007/JHEP12(2012)061, arXiv:1209.6215.
- [54] J. Pumplin et al., “New generation of parton distributions with uncertainties from global QCD analysis”, *JHEP* **07** (2002) 012, doi:10.1088/1126-6708/2002/07/012, arXiv:hep-ph/0201195.
- [55] H.-L. Lai et al., “New parton distributions for collider physics”, *Phys. Rev. D* **82** (2010) 074024, doi:10.1103/PhysRevD.82.074024, arXiv:1007.2241.
- [56] NNPDF Collaboration, “Parton distributions for the LHC run II”, *JHEP* **04** (2015) 040, doi:10.1007/JHEP04(2015)040, arXiv:1410.8849.
- [57] T. Sjöstrand, S. Mrenna, and P. Z. Skands, “A brief introduction to PYTHIA 8.1”, *Comput. Phys. Commun.* **178** (2008) 852, doi:10.1016/j.cpc.2008.01.036, arXiv:0710.3820.
- [58] CMS Collaboration, “Study of the underlying event at forward rapidity in pp collisions at $\sqrt{s} = 0.9, 2.76,$ and 7 TeV”, *JHEP* **04** (2013) 072, doi:10.1007/JHEP04(2013)072, arXiv:1302.2394.
- [59] CMS Collaboration, “Event generator tunes obtained from underlying event and multiparton scattering measurements”, *Eur. Phys. J. C* **76** (2016) 155, doi:10.1140/epjc/s10052-016-3988-x, arXiv:1512.00815.
- [60] LHC Higgs Cross Section Working Group, “Handbook of LHC Higgs cross sections: 4. deciphering the nature of the Higgs sector”, CERN (2016) doi:10.23731/CYRM-2017-002, arXiv:1610.07922.
- [61] GEANT4 Collaboration, “GEANT4—a simulation toolkit”, *Nucl. Instrum. Meth. A* **506** (2003) 250, doi:10.1016/S0168-9002(03)01368-8.
- [62] T. Gleisberg et al., “Event generation with SHERPA 1.1”, *JHEP* **02** (2009) 007, doi:10.1088/1126-6708/2009/02/007, arXiv:0811.4622.
- [63] E. Re, “NLO corrections merged with parton showers for Z+2 jets production using the POWHEG method”, *JHEP* **10** (2012) 031, doi:10.1007/JHEP10(2012)031, arXiv:1204.5433.
- [64] CMS Collaboration, “Particle-flow reconstruction and global event description with the CMS detector”, *JINST* **12** (2017) P10003, doi:10.1088/1748-0221/12/10/P10003, arXiv:1706.04965.
- [65] CMS Collaboration, “Energy calibration and resolution of the CMS electromagnetic calorimeter in pp collisions at $\sqrt{s} = 7$ TeV”, *JINST* **8** (2013) P09009, doi:10.1088/1748-0221/8/09/P09009, arXiv:1306.2016.
- [66] P. D. Dauncey, M. Kenzie, N. Wardle, and G. J. Davies, “Handling uncertainties in background shapes: the discrete profiling method”, *JINST* **10** (2015) P04015, doi:10.1088/1748-0221/10/04/P04015, arXiv:1408.6865.

- [67] M. Oreglia, "A study of the reactions $\psi' \rightarrow \gamma\gamma\psi$ ". PhD thesis, Stanford University, 1980. SLAC Report SLAC-R-236.
- [68] R. A. Fisher, "On the interpretation of χ^2 from contingency tables, and the calculation of p ", *J. Royal Stat. Soc* **85** (1922) 87, doi:10.2307/2340521.
- [69] CMS Collaboration, "CMS luminosity based on pixel cluster counting - Summer 2013 update", CMS Physics Analysis Summary CMS-PAS-LUM-13-001, 2013.
- [70] CMS Collaboration, "CMS luminosity measurements for the 2016 data taking period", CMS Physics Analysis Summary CMS-PAS-LUM-17-001, 2017.
- [71] S. Carrazza et al., "An unbiased Hessian representation for Monte Carlo PDFs", *Eur. Phys. J. C* **75** (2015) 369, doi:10.1140/epjc/s10052-015-3590-7, arXiv:1505.06736.
- [72] J. Butterworth et al., "PDF4LHC recommendations for LHC Run II", *J. Phys. G* **43** (2016) 023001, doi:10.1088/0954-3899/43/2/023001, arXiv:1510.03865.
- [73] ATLAS and CMS Collaborations, LHC Higgs Combination Group, "Procedure for the LHC Higgs boson search combination in Summer 2011", Technical Report CMS-NOTE-2011-005, ATL-PHYS-PUB-2011-11, CERN, 2011.
- [74] T. Junk, "Confidence level computation for combining searches with small statistics", *Nucl. Instrum. Meth. A* **434** (1999) 435, doi:10.1016/S0168-9002(99)00498-2, arXiv:hep-ex/9902006.
- [75] A. L. Read, "Presentation of search results: The CL(s) technique", *J. Phys. G* **28** (2002) 2693, doi:10.1088/0954-3899/28/10/313.
- [76] G. Cowan, K. Cranmer, E. Gross, and O. Vitells, "Asymptotic formulae for likelihood-based tests of new physics", *Eur. Phys. J. C* **71** (2011) 1554, doi:10.1140/epjc/s10052-011-1554-0, arXiv:1007.1727. [Erratum: doi:10.1140/epjc/s10052-013-2501-z].
- [77] E. Gross and O. Vitells, "Trial factors for the look elsewhere effect in high energy physics", *Eur. Phys. J. C* **70** (2010) 525, doi:10.1140/epjc/s10052-010-1470-8, arXiv:1005.1891.

A The CMS Collaboration

Yerevan Physics Institute, Yerevan, Armenia

A.M. Sirunyan, A. Tumasyan

Institut für Hochenergiephysik, Wien, Austria

W. Adam, F. Ambrogio, E. Asilar, T. Bergauer, J. Brandstetter, E. Brondolin, M. Dragicevic, J. Erö, A. Escalante Del Valle, M. Flechl, M. Friedl, R. Frühwirth¹, V.M. Ghete, J. Hrubec, M. Jeitler¹, N. Krammer, I. Krätschmer, D. Liko, T. Madlener, I. Mikulec, N. Rad, H. Rohringer, J. Schieck¹, R. Schöfbeck, M. Spanring, D. Spitzbart, A. Taurok, W. Waltenberger, J. Wittmann, C.-E. Wulz¹, M. Zarucki

Institute for Nuclear Problems, Minsk, Belarus

V. Chekhovsky, V. Mossolov, J. Suarez Gonzalez

Universiteit Antwerpen, Antwerpen, Belgium

E.A. De Wolf, D. Di Croce, X. Janssen, J. Lauwers, M. Pieters, M. Van De Klundert, H. Van Haevermaet, P. Van Mechelen, N. Van Remortel

Vrije Universiteit Brussel, Brussel, Belgium

S. Abu Zeid, F. Blekman, J. D'Hondt, I. De Bruyn, J. De Clercq, K. Deroover, G. Flouris, D. Lontkovskyi, S. Lowette, I. Marchesini, S. Moortgat, L. Moreels, Q. Python, K. Skovpen, S. Tavernier, W. Van Doninck, P. Van Mulders, I. Van Parijs

Université Libre de Bruxelles, Bruxelles, Belgium

D. Beghin, B. Bilin, H. Brun, B. Clerbaux, G. De Lentdecker, H. Delannoy, B. Dorney, G. Fasanella, L. Favart, R. Goldouzian, A. Grebenyuk, A.K. Kalsi, T. Lenzi, J. Luetic, T. Seva, E. Starling, C. Vander Velde, P. Vanlaer, D. Vannerom, R. Yonamine

Ghent University, Ghent, Belgium

T. Cornelis, D. Dobur, A. Fagot, M. Gul, I. Khvastunov², D. Poyraz, C. Roskas, D. Trocino, M. Tytgat, W. Verbeke, B. Vermassen, M. Vit, N. Zaganidis

Université Catholique de Louvain, Louvain-la-Neuve, Belgium

H. Bakhshiansohi, O. Bondu, S. Brochet, G. Bruno, C. Caputo, A. Caudron, P. David, S. De Visscher, C. Delaere, M. Delcourt, B. Francois, A. Giammanco, G. Krintiras, V. Lemaitre, A. Magitteri, A. Mertens, M. Musich, K. Piotrkowski, L. Quertenmont, A. Saggio, M. Vidal Marono, S. Wertz, J. Zobec

Centro Brasileiro de Pesquisas Físicas, Rio de Janeiro, Brazil

W.L. Aldá Júnior, F.L. Alves, G.A. Alves, L. Brito, G. Correia Silva, C. Hensel, A. Moraes, M.E. Pol, P. Rebello Teles

Universidade do Estado do Rio de Janeiro, Rio de Janeiro, Brazil

E. Belchior Batista Das Chagas, W. Carvalho, J. Chinellato³, E. Coelho, E.M. Da Costa, G.G. Da Silveira⁴, D. De Jesus Damiao, S. Fonseca De Souza, H. Malbouisson, M. Medina Jaime⁵, M. Melo De Almeida, C. Mora Herrera, L. Mundim, H. Nogima, L.J. Sanchez Rosas, A. Santoro, A. Sznajder, M. Thiel, E.J. Tonelli Manganote³, F. Torres Da Silva De Araujo, A. Vilela Pereira

Universidade Estadual Paulista ^a, Universidade Federal do ABC ^b, São Paulo, Brazil

S. Ahuja^a, C.A. Bernardes^a, L. Calligaris^a, T.R. Fernandez Perez Tomei^a, E.M. Gregores^b, P.G. Mercadante^b, S.F. Novaes^a, SandraS. Padula^a, D. Romero Abad^b, J.C. Ruiz Vargas^a

Institute for Nuclear Research and Nuclear Energy, Bulgarian Academy of Sciences, Sofia, Bulgaria

A. Aleksandrov, R. Hadjiiska, P. Iaydjiev, A. Marinov, M. Misheva, M. Rodozov, M. Shopova, G. Sultanov

University of Sofia, Sofia, Bulgaria

A. Dimitrov, L. Litov, B. Pavlov, P. Petkov

Beihang University, Beijing, China

W. Fang⁶, X. Gao⁶, L. Yuan

Institute of High Energy Physics, Beijing, China

M. Ahmad, J.G. Bian, G.M. Chen, H.S. Chen, M. Chen, Y. Chen, C.H. Jiang, D. Leggat, H. Liao, Z. Liu, F. Romeo, S.M. Shaheen, A. Spiezia, J. Tao, C. Wang, Z. Wang, E. Yazgan, H. Zhang, J. Zhao

State Key Laboratory of Nuclear Physics and Technology, Peking University, Beijing, China

Y. Ban, G. Chen, J. Li, Q. Li, S. Liu, Y. Mao, S.J. Qian, D. Wang, Z. Xu

Tsinghua University, Beijing, China

Y. Wang

Universidad de Los Andes, Bogota, Colombia

C. Avila, A. Cabrera, C.A. Carrillo Montoya, L.F. Chaparro Sierra, C. Florez, C.F. González Hernández, M.A. Segura Delgado

University of Split, Faculty of Electrical Engineering, Mechanical Engineering and Naval Architecture, Split, Croatia

B. Courbon, N. Godinovic, D. Lelas, I. Puljak, T. Sculac

University of Split, Faculty of Science, Split, Croatia

Z. Antunovic, M. Kovac

Institute Rudjer Boskovic, Zagreb, Croatia

V. Brigljevic, D. Ferencek, K. Kadija, B. Mesic, A. Starodumov⁷, T. Susa

University of Cyprus, Nicosia, Cyprus

M.W. Ather, A. Attikis, G. Mavromanolakis, J. Mousa, C. Nicolaou, F. Ptochos, P.A. Razis, H. Rykaczewski

Charles University, Prague, Czech Republic

M. Finger⁸, M. Finger Jr.⁸

Universidad San Francisco de Quito, Quito, Ecuador

E. Carrera Jarrin

Academy of Scientific Research and Technology of the Arab Republic of Egypt, Egyptian Network of High Energy Physics, Cairo, Egypt

H. Abdalla⁹, A.A. Abdelalim^{10,11}, E. Salama^{12,13}

National Institute of Chemical Physics and Biophysics, Tallinn, Estonia

S. Bhowmik, A. Carvalho Antunes De Oliveira, R.K. Dewanjee, M. Kadastik, L. Perrini, M. Raidal, C. Veelken

Department of Physics, University of Helsinki, Helsinki, Finland

P. Eerola, H. Kirschenmann, J. Pekkanen, M. Voutilainen

Helsinki Institute of Physics, Helsinki, Finland

J. Havukainen, J.K. Heikkilä, T. Järvinen, V. Karimäki, R. Kinnunen, T. Lampén, K. Lassila-Perini, S. Laurila, S. Lehti, T. Lindén, P. Luukka, T. Mäenpää, H. Siikonen, E. Tuominen, J. Tuominiemi

Lappeenranta University of Technology, Lappeenranta, Finland

T. Tuuva

IRFU, CEA, Université Paris-Saclay, Gif-sur-Yvette, France

M. Besancon, F. Couderc, M. Dejardin, D. Denegri, J.L. Faure, F. Ferri, S. Ganjour, A. Givernaud, P. Gras, G. Hamel de Monchenault, P. Jarry, C. Leloup, E. Locci, M. Machet, J. Malcles, G. Negro, J. Rander, A. Rosowsky, M.Ö. Sahin, M. Titov

Laboratoire Leprince-Ringuet, Ecole polytechnique, CNRS/IN2P3, Université Paris-Saclay, Palaiseau, France

A. Abdulsalam¹⁴, C. Amendola, I. Antropov, S. Baffioni, F. Beaudette, P. Busson, L. Cadamuro, C. Charlot, R. Granier de Cassagnac, M. Jo, I. Kucher, S. Lisniak, A. Lobanov, J. Martin Blanco, M. Nguyen, C. Ochando, G. Ortona, P. Paganini, P. Pigard, R. Salerno, J.B. Sauvan, Y. Sirois, A.G. Stahl Leiton, Y. Yilmaz, A. Zabi, A. Zghiche

Université de Strasbourg, CNRS, IPHC UMR 7178, Strasbourg, France

J.-L. Agram¹⁵, J. Andrea, D. Bloch, J.-M. Brom, E.C. Chabert, C. Collard, E. Conte¹⁵, X. Coubez, F. Drouhin¹⁵, J.-C. Fontaine¹⁵, D. Gelé, U. Goerlach, M. Jansová, P. Juillot, A.-C. Le Bihan, N. Tonon, P. Van Hove

Centre de Calcul de l'Institut National de Physique Nucleaire et de Physique des Particules, CNRS/IN2P3, Villeurbanne, France

S. Gadrat

Université de Lyon, Université Claude Bernard Lyon 1, CNRS-IN2P3, Institut de Physique Nucléaire de Lyon, Villeurbanne, France

S. Beauceron, C. Bernet, G. Boudoul, N. Chanon, R. Chierici, D. Contardo, P. Depasse, H. El Mamouni, J. Fay, L. Finco, S. Gascon, M. Gouzevitch, G. Grenier, B. Ille, F. Lagarde, I.B. Laktineh, H. Lattaud, M. Lethuillier, L. Mirabito, A.L. Pequegnot, S. Perries, A. Popov¹⁶, V. Sordini, M. Vander Donckt, S. Viret, S. Zhang

Georgian Technical University, Tbilisi, Georgia

T. Toriashvili¹⁷

Tbilisi State University, Tbilisi, Georgia

Z. Tsamalaidze⁸

RWTH Aachen University, I. Physikalisches Institut, Aachen, Germany

C. Autermann, L. Feld, M.K. Kiesel, K. Klein, M. Lipinski, M. Preuten, M.P. Rauch, C. Schomakers, J. Schulz, M. Teroerde, B. Wittmer, V. Zhukov¹⁶

RWTH Aachen University, III. Physikalisches Institut A, Aachen, Germany

A. Albert, D. Duchardt, M. Endres, M. Erdmann, S. Erdweg, T. Esch, R. Fischer, S. Ghosh, A. Güth, T. Hebbeker, C. Heidemann, K. Hoepfner, S. Knutzen, M. Merschmeyer, A. Meyer, P. Millet, S. Mukherjee, T. Pook, M. Radziej, H. Reithler, M. Rieger, F. Scheuch, D. Teyssier, S. Thüer

RWTH Aachen University, III. Physikalisches Institut B, Aachen, Germany

G. Flügge, B. Kargoll, T. Kress, A. Künsken, T. Müller, A. Nehr Korn, A. Nowack, C. Pistone, O. Pooth, A. Stahl¹⁸

Deutsches Elektronen-Synchrotron, Hamburg, Germany

M. Aldaya Martin, T. Arndt, C. Asawatangtrakuldee, I. Babounikau, K. Beernaert, O. Behnke, U. Behrens, A. Bermúdez Martínez, D. Bertsche, A.A. Bin Anuar, K. Borras¹⁹, V. Botta, A. Campbell, P. Connor, C. Contreras-Campana, F. Costanza, V. Danilov, A. De Wit, C. Diez Pardos, D. Domínguez Damiani, G. Eckerlin, D. Eckstein, T. Eichhorn, A. Elwood, E. Eren, E. Gallo²⁰, A. Geiser, J.M. Grados Luyando, A. Grohsjean, P. Gunnellini, M. Guthoff, A. Harb, J. Hauk, H. Jung, M. Kasemann, J. Keaveney, C. Kleinwort, J. Knolle, D. Krücker, W. Lange, A. Lelek, T. Lenz, K. Lipka, W. Lohmann²¹, R. Mankel, I.-A. Melzer-Pellmann, A.B. Meyer, M. Meyer, M. Missiroli, G. Mittag, J. Mnich, A. Mussgiller, S.K. Pflitsch, D. Pitzl, A. Raspereza, M. Savitskyi, P. Saxena, C. Schwanenberger, R. Shevchenko, A. Singh, N. Stefaniuk, H. Tholen, G.P. Van Onsem, R. Walsh, Y. Wen, K. Wichmann, C. Wissing, O. Zenaiev

University of Hamburg, Hamburg, Germany

R. Aggleton, S. Bein, A. Benecke, V. Blobel, M. Centis Vignali, T. Dreyer, E. Garutti, D. Gonzalez, J. Haller, A. Hinzmann, M. Hoffmann, A. Karavdina, G. Kasieczka, R. Klanner, R. Kogler, N. Kovalchuk, S. Kurz, V. Kutzner, J. Lange, D. Marconi, J. Multhaupt, M. Niedziela, D. Nowatschin, T. Peiffer, A. Perieanu, A. Reimers, C. Scharf, P. Schleper, A. Schmidt, S. Schumann, J. Schwandt, J. Sonneveld, H. Stadie, G. Steinbrück, F.M. Stober, M. Stöver, D. Troendle, E. Usai, A. Vanhoefer, B. Vormwald

Karlsruher Institut fuer Technologie, Karlsruhe, Germany

M. Akbiyik, C. Barth, M. Baselga, S. Baur, E. Butz, R. Caspart, T. Chwalek, F. Colombo, W. De Boer, A. Dierlamm, N. Faltermann, B. Freund, R. Friese, M. Giffels, M.A. Harrendorf, F. Hartmann¹⁸, S.M. Heindl, U. Husemann, F. Kassel¹⁸, S. Kudella, H. Mildner, M.U. Mozer, Th. Müller, M. Plagge, G. Quast, K. Rabbertz, M. Schröder, I. Shvetsov, G. Sieber, H.J. Simonis, R. Ulrich, S. Wayand, M. Weber, T. Weiler, S. Williamson, C. Wöhrmann, R. Wolf

Institute of Nuclear and Particle Physics (INPP), NCSR Demokritos, Aghia Paraskevi, Greece

G. Anagnostou, G. Daskalakis, T. Gerasis, A. Kyriakis, D. Loukas, I. Topsis-Giotis

National and Kapodistrian University of Athens, Athens, Greece

G. Karathanasis, S. Kesisoglou, A. Panagiotou, N. Saoulidou, E. Tziaferi, K. Vellidis

National Technical University of Athens, Athens, Greece

K. Kousouris, I. Papakrivopoulos

University of Ioánnina, Ioánnina, Greece

I. Evangelou, C. Foudas, P. Gianneios, P. Katsoulis, P. Kokkas, S. Mallios, N. Manthos, I. Papadopoulos, E. Paradas, J. Strologas, F.A. Triantis, D. Tsitsonis

MTA-ELTE Lendület CMS Particle and Nuclear Physics Group, Eötvös Loránd University, Budapest, Hungary

M. Csanad, N. Filipovic, G. Pasztor, O. Surányi, G.I. Veres

Wigner Research Centre for Physics, Budapest, Hungary

G. Bencze, C. Hajdu, D. Horvath²², Á. Hunyadi, F. Sikler, T.Á. Vámi, V. Veszpremi, G. Vesztergombi[†]

Institute of Nuclear Research ATOMKI, Debrecen, Hungary

N. Beni, S. Czellar, J. Karancsi²⁴, A. Makovec, J. Molnar, Z. Szillasi

Institute of Physics, University of Debrecen, Debrecen, Hungary

M. Bartók²³, P. Raics, Z.L. Trocsanyi, B. Ujvari

Indian Institute of Science (IISc), Bangalore, India

S. Choudhury, J.R. Komaragiri

National Institute of Science Education and Research, HBNI, Bhubaneswar, India

S. Bahinipati²⁵, P. Mal, K. Mandal, A. Nayak²⁶, D.K. Sahoo²⁵, S.K. Swain

Panjab University, Chandigarh, India

S. Bansal, S.B. Beri, V. Bhatnagar, S. Chauhan, R. Chawla, N. Dhingra, R. Gupta, A. Kaur, M. Kaur, S. Kaur, R. Kumar, P. Kumari, M. Lohan, A. Mehta, S. Sharma, J.B. Singh, G. Walia

University of Delhi, Delhi, India

A. Bhardwaj, B.C. Choudhary, R.B. Garg, S. Keshri, A. Kumar, Ashok Kumar, S. Malhotra, M. Naimuddin, K. Ranjan, Aashaq Shah, R. Sharma

Saha Institute of Nuclear Physics, HBNI, Kolkata, India

R. Bhardwaj²⁷, R. Bhattacharya, S. Bhattacharya, U. Bhawandeep²⁷, D. Bhowmik, S. Dey, S. Dutt²⁷, S. Dutta, S. Ghosh, N. Majumdar, K. Mondal, S. Mukhopadhyay, S. Nandan, A. Purohit, P.K. Rout, A. Roy, S. Roy Chowdhury, S. Sarkar, M. Sharan, B. Singh, S. Thakur²⁷

Indian Institute of Technology Madras, Madras, India

P.K. Behera

Bhabha Atomic Research Centre, Mumbai, India

R. Chudasama, D. Dutta, V. Jha, V. Kumar, A.K. Mohanty¹⁸, P.K. Netrakanti, L.M. Pant, P. Shukla, A. Topkar

Tata Institute of Fundamental Research-A, Mumbai, India

T. Aziz, S. Dugad, B. Mahakud, S. Mitra, G.B. Mohanty, R. Ravindra Kumar Verma, N. Sur, B. Sutar

Tata Institute of Fundamental Research-B, Mumbai, India

S. Banerjee, S. Bhattacharya, S. Chatterjee, P. Das, M. Guchait, Sa. Jain, S. Kumar, M. Maity²⁸, G. Majumder, K. Mazumdar, N. Sahoo, T. Sarkar²⁸, N. Wickramage²⁹

Indian Institute of Science Education and Research (IISER), Pune, India

S. Chauhan, S. Dube, V. Hegde, A. Kapoor, K. Kothekar, S. Pandey, A. Rane, S. Sharma

Institute for Research in Fundamental Sciences (IPM), Tehran, Iran

S. Chenarani³⁰, E. Eskandari Tadavani, S.M. Etesami³⁰, M. Khakzad, M. Mohammadi Najafabadi, M. Naseri, S. Paktinat Mehdiabadi³¹, F. Rezaei Hosseinabadi, B. Safarzadeh³², M. Zeinali

University College Dublin, Dublin, Ireland

M. Felcini, M. Grunewald

INFN Sezione di Bari ^a, Università di Bari ^b, Politecnico di Bari ^c, Bari, Italy

M. Abbrescia^{a,b}, C. Calabria^{a,b}, A. Colaleo^a, D. Creanza^{a,c}, L. Cristella^{a,b}, N. De Filippis^{a,c}, M. De Palma^{a,b}, A. Di Florio^{a,b}, F. Errico^{a,b}, L. Fiore^a, A. Gelmi^{a,b}, G. Iaselli^{a,c}, S. Lezki^{a,b}, G. Maggi^{a,c}, M. Maggi^a, B. Marangelli^{a,b}, G. Miniello^{a,b}, S. My^{a,b}, S. Nuzzo^{a,b}, A. Pompili^{a,b}, G. Pugliese^{a,c}, R. Radogna^a, A. Ranieri^a, G. Selvaggi^{a,b}, A. Sharma^a, L. Silvestris^{a,18}, R. Venditti^a, P. Verwilligen^a, G. Zito^a

INFN Sezione di Bologna ^a, Università di Bologna ^b, Bologna, Italy

G. Abbiendi^a, C. Battilana^{a,b}, D. Bonacorsi^{a,b}, L. Borgonovi^{a,b}, S. Braibant-Giacomelli^{a,b}, L. Brigliadori^{a,b}, R. Campanini^{a,b}, P. Capiluppi^{a,b}, A. Castro^{a,b}, F.R. Cavallo^a, S.S. Chhibra^{a,b}, G. Codispoti^{a,b}, M. Cuffiani^{a,b}, G.M. Dallavalle^a, F. Fabbri^a, A. Fanfani^{a,b}, D. Fasanella^{a,b}, P. Giacomelli^a, C. Grandi^a, L. Guiducci^{a,b}, S. Marcellini^a, G. Masetti^a, A. Montanari^a, F.L. Navarria^{a,b}, A. Perrotta^a, A.M. Rossi^{a,b}, T. Rovelli^{a,b}, G.P. Siroli^{a,b}, N. Tosi^a

INFN Sezione di Catania ^a, Università di Catania ^b, Catania, Italy

S. Albergo^{a,b}, S. Costa^{a,b}, A. Di Mattia^a, F. Giordano^{a,b}, R. Potenza^{a,b}, A. Tricomi^{a,b}, C. Tuve^{a,b}

INFN Sezione di Firenze ^a, Università di Firenze ^b, Firenze, Italy

G. Barbagli^a, K. Chatterjee^{a,b}, V. Ciulli^{a,b}, C. Civinini^a, R. D'Alessandro^{a,b}, E. Focardi^{a,b}, G. Latino, P. Lenzi^{a,b}, M. Meschini^a, S. Paoletti^a, L. Russo^{a,33}, G. Sguazzoni^a, D. Strom^a, L. Viliani^a

INFN Laboratori Nazionali di Frascati, Frascati, Italy

L. Benussi, S. Bianco, F. Fabbri, D. Piccolo, F. Primavera¹⁸

INFN Sezione di Genova ^a, Università di Genova ^b, Genova, Italy

V. Calvelli, F. Ferro^a, F. Ravera^{a,b}, E. Robutti^a, S. Tosi^{a,b}

INFN Sezione di Milano-Bicocca ^a, Università di Milano-Bicocca ^b, Milano, Italy

A. Benaglia^a, A. Beschi^b, L. Brianza^{a,b}, F. Brivio^{a,b}, V. Ciriolo^{a,b,18}, M.E. Dinardo^{a,b}, S. Fiorendi^{a,b}, S. Gennai^a, A. Ghezzi^{a,b}, P. Govoni^{a,b}, M. Malberti^{a,b}, S. Malvezzi^a, R.A. Manzoni^{a,b}, D. Menasce^a, L. Moroni^a, M. Paganoni^{a,b}, K. Pauwels^{a,b}, D. Pedrini^a, S. Pigazzini^{a,b,34}, S. Ragazzi^{a,b}, T. Tabarelli de Fatis^{a,b}

INFN Sezione di Napoli ^a, Università di Napoli 'Federico II' ^b, Napoli, Italy, Università della Basilicata ^c, Potenza, Italy, Università G. Marconi ^d, Roma, Italy

S. Buontempo^a, N. Cavallo^{a,c}, S. Di Guida^{a,d,18}, F. Fabozzi^{a,c}, F. Fienga^{a,b}, G. Galati^{a,b}, A.O.M. Iorio^{a,b}, W.A. Khan^a, L. Lista^a, S. Meola^{a,d,18}, P. Paolucci^{a,18}, C. Sciacca^{a,b}, F. Thyssen^a, E. Voevodina^{a,b}

INFN Sezione di Padova ^a, Università di Padova ^b, Padova, Italy, Università di Trento ^c, Trento, Italy

P. Azzi^a, N. Bacchetta^a, L. Benato^{a,b}, A. Boletti^{a,b}, R. Carlin^{a,b}, P. Checchia^a, M. Dall'Osso^{a,b}, P. De Castro Manzano^a, T. Dorigo^a, U. Dosselli^a, F. Gasparini^{a,b}, U. Gasparini^{a,b}, A. Gozzelino^a, S. Lacaprara^a, P. Lujan, M. Margoni^{a,b}, A.T. Meneguzzo^{a,b}, N. Pozzobon^{a,b}, P. Ronchese^{a,b}, R. Rossin^{a,b}, F. Simonetto^{a,b}, A. Tiko, E. Torassa^a, S. Ventura^a, M. Zanetti^{a,b}, P. Zotto^{a,b}

INFN Sezione di Pavia ^a, Università di Pavia ^b, Pavia, Italy

A. Braghieri^a, A. Magnani^a, P. Montagna^{a,b}, S.P. Ratti^{a,b}, V. Re^a, M. Ressegotti^{a,b}, C. Riccardi^{a,b}, P. Salvini^a, I. Vai^{a,b}, P. Vitulo^{a,b}

INFN Sezione di Perugia ^a, Università di Perugia ^b, Perugia, Italy

L. Alunni Solestizi^{a,b}, M. Biasini^{a,b}, G.M. Bilei^a, C. Cecchi^{a,b}, D. Ciangottini^{a,b}, L. Fanò^{a,b}, P. Lariccia^{a,b}, R. Leonardi^{a,b}, E. Manoni^a, G. Mantovani^{a,b}, V. Mariani^{a,b}, M. Menichelli^a, A. Rossi^{a,b}, A. Santocchia^{a,b}, D. Spiga^a

INFN Sezione di Pisa ^a, Università di Pisa ^b, Scuola Normale Superiore di Pisa ^c, Pisa, Italy

K. Androsov^a, P. Azzurri^a, G. Bagliesi^a, L. Bianchini^a, T. Boccali^a, L. Borrello, R. Castaldi^a, M.A. Ciocci^{a,b}, R. Dell'Orso^a, G. Fedi^a, L. Giannini^{a,c}, A. Giassi^a, M.T. Grippo^a, F. Ligabue^{a,c}, T. Lomtadze^a, E. Manca^{a,c}, G. Mandorli^{a,c}, A. Messineo^{a,b}, F. Palla^a, A. Rizzi^{a,b}, P. Spagnolo^a, R. Tenchini^a, G. Tonelli^{a,b}, A. Venturi^a, P.G. Verdini^a

INFN Sezione di Roma ^a, Sapienza Università di Roma ^b, Rome, Italy

L. Barone^{a,b}, F. Cavallari^a, M. Cipriani^{a,b}, N. Daci^a, D. Del Re^{a,b}, E. Di Marco^{a,b}, M. Diemoz^a, S. Gelli^{a,b}, E. Longo^{a,b}, B. Marzocchi^{a,b}, P. Meridiani^a, G. Organtini^{a,b}, F. Pandolfi^a, R. Paramatti^{a,b}, F. Preiato^{a,b}, S. Rahatlou^{a,b}, C. Rovelli^a, F. Santanastasio^{a,b}

INFN Sezione di Torino ^a, Università di Torino ^b, Torino, Italy, Università del Piemonte Orientale ^c, Novara, Italy

N. Amapane^{a,b}, R. Arcidiacono^{a,c}, S. Argiro^{a,b}, M. Arneodo^{a,c}, N. Bartosik^a, R. Bellan^{a,b}, C. Biino^a, N. Cartiglia^a, R. Castello^{a,b}, F. Cenna^{a,b}, M. Costa^{a,b}, R. Covarelli^{a,b}, A. Degano^{a,b}, N. Demaria^a, B. Kiani^{a,b}, C. Mariotti^a, S. Maselli^a, E. Migliore^{a,b}, V. Monaco^{a,b}, E. Monteil^{a,b}, M. Monteno^a, M.M. Obertino^{a,b}, L. Pacher^{a,b}, N. Pastrone^a, M. Pelliccioni^a, G.L. Pinna Angioni^{a,b}, A. Romero^{a,b}, M. Ruspa^{a,c}, R. Sacchi^{a,b}, K. Shchelina^{a,b}, V. Sola^a, A. Solano^{a,b}, A. Staiano^a

INFN Sezione di Trieste ^a, Università di Trieste ^b, Trieste, Italy

S. Belforte^a, V. Candelise^{a,b}, M. Casarsa^a, F. Cossutti^a, G. Della Ricca^{a,b}, F. Vazzoler^{a,b}, A. Zanetti^a

Kyungpook National University, Daegu, Korea

D.H. Kim, G.N. Kim, M.S. Kim, J. Lee, S. Lee, S.W. Lee, C.S. Moon, Y.D. Oh, S. Sekmen, D.C. Son, Y.C. Yang

Chonnam National University, Institute for Universe and Elementary Particles, Kwangju, Korea

H. Kim, D.H. Moon, G. Oh

Hanyang University, Seoul, Korea

J.A. Brochero Cifuentes, J. Goh, T.J. Kim

Korea University, Seoul, Korea

S. Cho, S. Choi, Y. Go, D. Gyun, S. Ha, B. Hong, Y. Jo, Y. Kim, K. Lee, K.S. Lee, S. Lee, J. Lim, S.K. Park, Y. Roh

Seoul National University, Seoul, Korea

J. Almond, J. Kim, J.S. Kim, H. Lee, K. Lee, K. Nam, S.B. Oh, B.C. Radburn-Smith, S.h. Seo, U.K. Yang, H.D. Yoo, G.B. Yu

University of Seoul, Seoul, Korea

H. Kim, J.H. Kim, J.S.H. Lee, I.C. Park

Sungkyunkwan University, Suwon, Korea

Y. Choi, C. Hwang, J. Lee, I. Yu

Vilnius University, Vilnius, Lithuania

V. Dudenas, A. Juodagalvis, J. Vaitkus

National Centre for Particle Physics, Universiti Malaya, Kuala Lumpur, Malaysia

I. Ahmed, Z.A. Ibrahim, M.A.B. Md Ali³⁵, F. Mohamad Idris³⁶, W.A.T. Wan Abdullah, M.N. Yusli, Z. Zolkapli

Centro de Investigacion y de Estudios Avanzados del IPN, Mexico City, Mexico

H. Castilla-Valdez, E. De La Cruz-Burelo, M.C. Duran-Osuna, I. Heredia-De La Cruz³⁷, R. Lopez-Fernandez, J. Mejia Guisao, R.I. Rabadan-Trejo, G. Ramirez-Sanchez, R Reyes-Almanza, A. Sanchez-Hernandez

Universidad Iberoamericana, Mexico City, Mexico

S. Carrillo Moreno, C. Oropeza Barrera, F. Vazquez Valencia

Benemerita Universidad Autonoma de Puebla, Puebla, Mexico

J. Eysermans, I. Pedraza, H.A. Salazar Ibarguen, C. Uribe Estrada

Universidad Autónoma de San Luis Potosí, San Luis Potosí, Mexico

A. Morelos Pineda

University of Auckland, Auckland, New Zealand

D. Krofcheck

University of Canterbury, Christchurch, New Zealand

S. Bheesette, P.H. Butler

National Centre for Physics, Quaid-I-Azam University, Islamabad, Pakistan

A. Ahmad, M. Ahmad, Q. Hassan, H.R. Hoorani, A. Saddique, M.A. Shah, M. Shoaib, M. Waqas

National Centre for Nuclear Research, Swierk, Poland

H. Bialkowska, M. Bluj, B. Boimska, T. Frueboes, M. Górski, M. Kazana, K. Nawrocki, M. Szleper, P. Traczyk, P. Zalewski

Institute of Experimental Physics, Faculty of Physics, University of Warsaw, Warsaw, Poland

K. Bunkowski, A. Byzuk³⁸, K. Doroba, A. Kalinowski, M. Konecki, J. Krolikowski, M. Misiura, M. Olszewski, A. Pyskir, M. Walczak

Laboratório de Instrumentação e Física Experimental de Partículas, Lisboa, Portugal

P. Bargassa, C. Beirão Da Cruz E Silva, A. Di Francesco, P. Faccioli, B. Galinhas, M. Gallinaro, J. Hollar, N. Leonardo, L. Lloret Iglesias, M.V. Nemallapudi, J. Seixas, G. Strong, O. Toldaiev, D. Vadrucio, J. Varela

Joint Institute for Nuclear Research, Dubna, Russia

S. Afanasiev, V. Alexakhin, P. Bunin, M. Gavrilenko, A. Golunov, I. Golutvin, N. Gorbounov, V. Karjavin, A. Lanev, A. Malakhov, V. Matveev^{39,40}, P. Moisezenz, V. Palichik, V. Perelygin, M. Savina, S. Shmatov, V. Smirnov, N. Voytishin, A. Zarubin

Petersburg Nuclear Physics Institute, Gatchina (St. Petersburg), Russia

Y. Ivanov, V. Kim⁴¹, E. Kuznetsova⁴², P. Levchenko, V. Murzin, V. Oreshkin, I. Smirnov, D. Sosnov, V. Sulimov, L. Uvarov, S. Vavilov, A. Vorobyev

Institute for Nuclear Research, Moscow, Russia

Yu. Andreev, A. Dermenev, S. Gninenko, N. Golubev, A. Karneyeu, M. Kirsanov, N. Krasnikov, A. Pashenkov, D. Tlisov, A. Toropin

Institute for Theoretical and Experimental Physics, Moscow, Russia

V. Epshteyn, V. Gavrilo, N. Lychkovskaya, V. Popov, I. Pozdnyakov, G. Safronov, A. Spiridonov, A. Steppenov, V. Stolin, M. Toms, E. Vlasov, A. Zhokin

Moscow Institute of Physics and Technology, Moscow, Russia

T. Aushev, A. Bylinkin⁴⁰

National Research Nuclear University 'Moscow Engineering Physics Institute' (MEPhI), Moscow, Russia

R. Chistov⁴³, M. Danilov⁴³, P. Parygin, D. Philippov, S. Polikarpov, E. Tarkovskii

P.N. Lebedev Physical Institute, Moscow, Russia

V. Andreev, M. Azarkin⁴⁰, I. Dremin⁴⁰, M. Kirakosyan⁴⁰, S.V. Rusakov, A. Terkulov

Skobeltsyn Institute of Nuclear Physics, Lomonosov Moscow State University, Moscow, Russia

A. Baskakov, A. Belyaev, E. Boos, V. Bunichev, M. Dubinin⁴⁴, L. Dudko, A. Ershov, A. Gribushin, V. Klyukhin, O. Kodolova, I. Lokhtin, I. Miagkov, S. Obraztsov, S. Petrushanko, V. Savrin

Novosibirsk State University (NSU), Novosibirsk, Russia

V. Blinov⁴⁵, D. Shtol⁴⁵, Y. Skovpen⁴⁵

Institute for High Energy Physics of National Research Centre 'Kurchatov Institute', Protvino, Russia

I. Azhgirey, I. Bayshev, S. Bitioukov, D. Elumakhov, A. Godizov, V. Kachanov, A. Kalinin, D. Konstantinov, P. Mandrik, V. Petrov, R. Ryutin, A. Sobol, S. Troshin, N. Tyurin, A. Uzunian, A. Volkov

National Research Tomsk Polytechnic University, Tomsk, Russia

A. Babaev

University of Belgrade, Faculty of Physics and Vinca Institute of Nuclear Sciences, Belgrade, Serbia

P. Adzic⁴⁶, P. Cirkovic, D. Devetak, M. Dordevic, J. Milosevic

Centro de Investigaciones Energéticas Medioambientales y Tecnológicas (CIEMAT), Madrid, Spain

J. Alcaraz Maestre, A. Álvarez Fernández, I. Bachiller, M. Barrio Luna, M. Cerrada, N. Colino, B. De La Cruz, A. Delgado Peris, C. Fernandez Bedoya, J.P. Fernández Ramos, J. Flix, M.C. Fouz, O. Gonzalez Lopez, S. Goy Lopez, J.M. Hernandez, M.I. Josa, D. Moran, A. Pérez-Calero Yzquierdo, J. Puerta Pelayo, I. Redondo, L. Romero, M.S. Soares, A. Triossi

Universidad Autónoma de Madrid, Madrid, Spain

C. Albajar, J.F. de Trocóniz

Universidad de Oviedo, Oviedo, Spain

J. Cuevas, C. Erice, J. Fernandez Menendez, S. Folgueras, I. Gonzalez Caballero, J.R. González Fernández, E. Palencia Cortezon, S. Sanchez Cruz, P. Vischia, J.M. Vizán García

Instituto de Física de Cantabria (IFCA), CSIC-Universidad de Cantabria, Santander, Spain

I.J. Cabrillo, A. Calderon, B. Chazin Quero, J. Duarte Campderros, M. Fernandez, P.J. Fernández Manteca, A. García Alonso, J. Garcia-Ferrero, G. Gomez, A. Lopez Virto, J. Marco, C. Martinez Rivero, P. Martinez Ruiz del Arbol, F. Matorras, J. Piedra Gomez, C. Prieels, T. Rodrigo, A. Ruiz-Jimeno, L. Scodellaro, N. Trevisani, I. Vila, R. Vilar Cortabitarte

CERN, European Organization for Nuclear Research, Geneva, Switzerland

D. Abbaneo, B. Akgun, E. Auffray, P. Baillon, A.H. Ball, D. Barney, J. Bendavid, M. Bianco, A. Bocci, C. Botta, T. Camporesi, M. Cepeda, G. Cerminara, E. Chapon, Y. Chen, D. d'Enterria, A. Dabrowski, V. Daponte, A. David, M. De Gruttola, A. De Roeck, N. Deelen, M. Dobson, T. du Pree, M. Dünser, N. Dupont, A. Elliott-Peisert, P. Everaerts, F. Fallavollita⁴⁷, G. Franzoni, J. Fulcher, W. Funk, D. Gigi, A. Gilbert, K. Gill, F. Glege, D. Gulhan, J. Hegeman, V. Innocente, A. Jafari, P. Janot, O. Karacheban²¹, J. Kieseler, V. Knünz, A. Kornmayer, M. Kramer¹, C. Lange, P. Lecoq, C. Lourenço, M.T. Lucchini, L. Malgeri, M. Mannelli, A. Martelli, F. Meijers, J.A. Merlin, S. Mersi, E. Meschi, P. Milenovic⁴⁸, F. Moortgat, M. Mulders, H. Neugebauer, J. Ngadiuba, S. Orfanelli, L. Orsini, F. Pantaleo¹⁸, L. Pape, E. Perez, M. Peruzzi, A. Petrilli, G. Petrucciani, A. Pfeiffer, M. Pierini, F.M. Pitters, D. Rabady, A. Racz, T. Reis, G. Rolandi⁴⁹, M. Rovere, H. Sakulin, C. Schäfer, C. Schwick, M. Seidel, M. Selvaggi, A. Sharma, P. Silva,

P. Sphicas⁵⁰, A. Stakia, J. Steggemann, M. Stoye, M. Tosi, D. Treille, A. Tsirou, V. Veckalns⁵¹, M. Verweij, W.D. Zeuner

Paul Scherrer Institut, Villigen, Switzerland

W. Bertl[†], L. Caminada⁵², K. Deiters, W. Erdmann, R. Horisberger, Q. Ingram, H.C. Kaestli, D. Kotlinski, U. Langenegger, T. Rohe, S.A. Wiederkehr

ETH Zurich - Institute for Particle Physics and Astrophysics (IPA), Zurich, Switzerland

M. Backhaus, L. Bäni, P. Berger, B. Casal, N. Chernyavskaya, G. Dissertori, M. Dittmar, M. Donegà, C. Dorfer, C. Grab, C. Heidegger, D. Hits, J. Hoss, T. Klijnsma, W. Luster, M. Marionneau, M.T. Meinhard, D. Meister, F. Micheli, P. Musella, F. Nessi-Tedaldi, J. Pata, F. Pauss, G. Perrin, L. Perrozzi, M. Quittnat, M. Reichmann, D. Ruini, D.A. Sanz Becerra, M. Schönenberger, L. Shchutska, V.R. Tavolaro, K. Theofilatos, M.L. Vesterbacka Olsson, R. Wallny, D.H. Zhu

Universität Zürich, Zurich, Switzerland

T.K. Aarrestad, C. Amsler⁵³, D. Brzhechko, M.F. Canelli, A. De Cosa, R. Del Burgo, S. Donato, C. Galloni, T. Hreus, B. Kilminster, I. Neutelings, D. Pinna, G. Rauco, P. Robmann, D. Salerno, K. Schweiger, C. Seitz, Y. Takahashi, A. Zucchetta

National Central University, Chung-Li, Taiwan

Y.H. Chang, K.y. Cheng, T.H. Doan, Sh. Jain, R. Khurana, C.M. Kuo, W. Lin, A. Pozdnyakov, S.S. Yu

National Taiwan University (NTU), Taipei, Taiwan

P. Chang, Y. Chao, K.F. Chen, P.H. Chen, F. Fiori, W.-S. Hou, Y. Hsiung, Arun Kumar, Y.F. Liu, R.-S. Lu, E. Paganis, A. Psallidas, A. Steen, J.f. Tsai

Chulalongkorn University, Faculty of Science, Department of Physics, Bangkok, Thailand

B. Asavapibhop, K. Kovitanggoon, G. Singh, N. Srimanobhas

Çukurova University, Physics Department, Science and Art Faculty, Adana, Turkey

A. Bat, F. Boran, S. Cerci⁵⁴, S. Damarseckin, Z.S. Demiroglu, C. Dozen, I. Dumanoglu, S. Girgis, G. Gokbulut, Y. Guler, I. Hos⁵⁵, E.E. Kangal⁵⁶, O. Kara, A. Kayis Topaksu, U. Kiminsu, M. Oglakci, G. Onengut, K. Ozdemir⁵⁷, D. Sunar Cerci⁵⁴, B. Tali⁵⁴, U.G. Tok, S. Turkcapar, I.S. Zorbakir, C. Zorbilmez

Middle East Technical University, Physics Department, Ankara, Turkey

G. Karapinar⁵⁸, K. Ocalan⁵⁹, M. Yalvac, M. Zeyrek

Bogazici University, Istanbul, Turkey

I.O. Atakisi, E. Gülmez, M. Kaya⁶⁰, O. Kaya⁶¹, S. Tekten, E.A. Yetkin⁶²

Istanbul Technical University, Istanbul, Turkey

M.N. Agaras, S. Atay, A. Cakir, K. Cankocak, Y. Komurcu

Institute for Scintillation Materials of National Academy of Science of Ukraine, Kharkov, Ukraine

B. Grynyov

National Scientific Center, Kharkov Institute of Physics and Technology, Kharkov, Ukraine

L. Levchuk

University of Bristol, Bristol, United Kingdom

F. Ball, L. Beck, J.J. Brooke, D. Burns, E. Clement, D. Cussans, O. Davignon, H. Flacher,

J. Goldstein, G.P. Heath, H.F. Heath, L. Kreczko, D.M. Newbold⁶³, S. Paramesvaran, T. Sakuma, S. Seif El Nasr-storey, D. Smith, V.J. Smith

Rutherford Appleton Laboratory, Didcot, United Kingdom

K.W. Bell, A. Belyaev⁶⁴, C. Brew, R.M. Brown, D. Cieri, D.J.A. Cockerill, J.A. Coughlan, K. Harder, S. Harper, J. Linacre, E. Olaiya, D. Petyt, C.H. Shepherd-Themistocleous, A. Thea, I.R. Tomalin, T. Williams, W.J. Womersley

Imperial College, London, United Kingdom

G. Auzinger, R. Bainbridge, P. Bloch, J. Borg, S. Breeze, O. Buchmuller, A. Bundock, S. Casasso, D. Colling, L. Corpe, P. Dauncey, G. Davies, M. Della Negra, R. Di Maria, Y. Haddad, G. Hall, G. Iles, T. James, M. Komm, R. Lane, C. Laner, L. Lyons, A.-M. Magnan, S. Malik, L. Mastrolorenzo, T. Matsushita, J. Nash⁶⁵, A. Nikitenko⁷, V. Palladino, M. Pesaresi, A. Richards, A. Rose, E. Scott, C. Seez, A. Shtipliyski, T. Strebler, S. Summers, A. Tapper, K. Uchida, M. Vazquez Acosta⁶⁶, T. Virdee¹⁸, N. Wardle, D. Winterbottom, J. Wright, S.C. Zenz

Brunel University, Uxbridge, United Kingdom

J.E. Cole, P.R. Hobson, A. Khan, P. Kyberd, C.K. Mackay, A. Morton, I.D. Reid, L. Teodorescu, S. Zahid

Baylor University, Waco, USA

A. Borzou, K. Call, J. Dittmann, K. Hatakeyama, H. Liu, N. Pastika, C. Smith

Catholic University of America, Washington, DC, USA

R. Bartek, A. Dominguez

The University of Alabama, Tuscaloosa, USA

A. Buccilli, S.I. Cooper, C. Henderson, P. Rumerio, C. West

Boston University, Boston, USA

D. Arcaro, A. Avetisyan, T. Bose, D. Gastler, D. Rankin, C. Richardson, J. Rohlf, L. Sulak, D. Zou

Brown University, Providence, USA

G. Benelli, D. Cutts, M. Hadley, J. Hakala, U. Heintz, J.M. Hogan⁶⁷, K.H.M. Kwok, E. Laird, G. Landsberg, J. Lee, Z. Mao, M. Narain, J. Pazzini, S. Piperov, S. Sagir, R. Syarif, D. Yu

University of California, Davis, Davis, USA

R. Band, C. Brainerd, R. Breedon, D. Burns, M. Calderon De La Barca Sanchez, M. Chertok, J. Conway, R. Conway, P.T. Cox, R. Erbacher, C. Flores, G. Funk, W. Ko, R. Lander, C. Mclean, M. Mulhearn, D. Pellett, J. Pilot, S. Shalhout, M. Shi, J. Smith, D. Stolp, D. Taylor, K. Tos, M. Tripathi, Z. Wang, F. Zhang

University of California, Los Angeles, USA

M. Bachtis, C. Bravo, R. Cousins, A. Dasgupta, A. Florent, J. Hauser, M. Ignatenko, N. Mccoll, S. Regnard, D. Saltzberg, C. Schnaible, V. Valuev

University of California, Riverside, Riverside, USA

E. Bouvier, K. Burt, R. Clare, J. Ellison, J.W. Gary, S.M.A. Ghiasi Shirazi, G. Hanson, G. Karapostoli, E. Kennedy, F. Lacroix, O.R. Long, M. Olmedo Negrete, M.I. Paneva, W. Si, L. Wang, H. Wei, S. Wimpenny, B.R. Yates

University of California, San Diego, La Jolla, USA

J.G. Branson, S. Cittolin, M. Derdzinski, R. Gerosa, D. Gilbert, B. Hashemi, A. Holzner, D. Klein, G. Kole, V. Krutelyov, J. Letts, M. Masciovecchio, D. Olivito, S. Padhi, M. Pieri, M. Sani,

V. Sharma, S. Simon, M. Tadel, A. Vartak, S. Wasserbaech⁶⁸, J. Wood, F. Würthwein, A. Yagil, G. Zevi Della Porta

University of California, Santa Barbara - Department of Physics, Santa Barbara, USA

N. Amin, R. Bhandari, J. Bradmiller-Feld, C. Campagnari, M. Citron, A. Dishaw, V. Dutta, M. Franco Sevilla, L. Gouskos, R. Heller, J. Incandela, A. Ovcharova, H. Qu, J. Richman, D. Stuart, I. Suarez, J. Yoo

California Institute of Technology, Pasadena, USA

D. Anderson, A. Bornheim, J. Bunn, J.M. Lawhorn, H.B. Newman, T.Q. Nguyen, C. Pena, M. Spiropulu, J.R. Vlimant, R. Wilkinson, S. Xie, Z. Zhang, R.Y. Zhu

Carnegie Mellon University, Pittsburgh, USA

M.B. Andrews, T. Ferguson, T. Mudholkar, M. Paulini, J. Russ, M. Sun, H. Vogel, I. Vorobiev, M. Weinberg

University of Colorado Boulder, Boulder, USA

J.P. Cumalat, W.T. Ford, F. Jensen, A. Johnson, M. Krohn, S. Leontsinis, E. MacDonald, T. Mulholland, K. Stenson, K.A. Ulmer, S.R. Wagner

Cornell University, Ithaca, USA

J. Alexander, J. Chaves, Y. Cheng, J. Chu, A. Datta, K. Mcdermott, N. Mirman, J.R. Patterson, D. Quach, A. Rinkevicius, A. Ryd, L. Skinnari, L. Soffi, S.M. Tan, Z. Tao, J. Thom, J. Tucker, P. Wittich, M. Zientek

Fermi National Accelerator Laboratory, Batavia, USA

S. Abdullin, M. Albrow, M. Alyari, G. Apollinari, A. Apresyan, A. Apyan, S. Banerjee, L.A.T. Bauerdick, A. Beretvas, J. Berryhill, P.C. Bhat, G. Bolla[†], K. Burkett, J.N. Butler, A. Canepa, G.B. Cerati, H.W.K. Cheung, F. Chlebana, M. Cremonesi, J. Duarte, V.D. Elvira, J. Freeman, Z. Gecse, E. Gottschalk, L. Gray, D. Green, S. Grünendahl, O. Gutsche, J. Hanlon, R.M. Harris, S. Hasegawa, J. Hirschauer, Z. Hu, B. Jayatilaka, S. Jindariani, M. Johnson, U. Joshi, B. Klima, M.J. Kortelainen, B. Kreis, S. Lammel, D. Lincoln, R. Lipton, M. Liu, T. Liu, R. Lopes De Sá, J. Lykken, K. Maeshima, N. Magini, J.M. Marraffino, D. Mason, P. McBride, P. Merkel, S. Mrenna, S. Nahn, V. O'Dell, K. Pedro, O. Prokofyev, G. Rakness, L. Ristori, A. Savoy-Navarro⁶⁹, B. Schneider, E. Sexton-Kennedy, A. Soha, W.J. Spalding, L. Spiegel, S. Stoynev, J. Strait, N. Strobbe, L. Taylor, S. Tkaczyk, N.V. Tran, L. Uplegger, E.W. Vaandering, C. Vernieri, M. Verzocchi, R. Vidal, M. Wang, H.A. Weber, A. Whitbeck, W. Wu

University of Florida, Gainesville, USA

D. Acosta, P. Avery, P. Bortignon, D. Bourilkov, A. Brinkerhoff, A. Carnes, M. Carver, D. Curry, R.D. Field, I.K. Furic, S.V. Gleyzer, B.M. Joshi, J. Konigsberg, A. Korytov, K. Kotov, P. Ma, K. Matchev, H. Mei, G. Mitselmakher, K. Shi, D. Sperka, N. Terentyev, L. Thomas, J. Wang, S. Wang, J. Yelton

Florida International University, Miami, USA

Y.R. Joshi, S. Linn, P. Markowitz, J.L. Rodriguez

Florida State University, Tallahassee, USA

A. Ackert, T. Adams, A. Askew, S. Hagopian, V. Hagopian, K.F. Johnson, T. Kolberg, G. Martinez, T. Perry, H. Prosper, A. Saha, A. Santra, V. Sharma, R. Yohay

Florida Institute of Technology, Melbourne, USA

M.M. Baarmand, V. Bhopatkar, S. Colafranceschi, M. Hohmann, D. Noonan, T. Roy, F. Yumiceva

University of Illinois at Chicago (UIC), Chicago, USA

M.R. Adams, L. Apanasevich, D. Berry, R.R. Betts, R. Cavanaugh, X. Chen, S. Dittmer, O. Evdokimov, C.E. Gerber, D.A. Hangal, D.J. Hofman, K. Jung, J. Kamin, I.D. Sandoval Gonzalez, M.B. Tonjes, N. Varelas, H. Wang, Z. Wu, J. Zhang

The University of Iowa, Iowa City, USA

B. Bilki⁷⁰, W. Clarida, K. Dilsiz⁷¹, S. Durgut, R.P. Gandrajula, M. Haytmyradov, V. Khristenko, J.-P. Merlo, H. Mermerkaya⁷², A. Mestvirishvili, A. Moeller, J. Nachtman, H. Ogul⁷³, Y. Onel, F. Ozok⁷⁴, A. Penzo, C. Snyder, E. Tiras, J. Wetzel, K. Yi

Johns Hopkins University, Baltimore, USA

B. Blumenfeld, A. Cocoros, N. Eminizer, D. Fehling, L. Feng, A.V. Gritsan, W.T. Hung, P. Maksimovic, J. Roskes, U. Sarica, M. Swartz, M. Xiao, C. You

The University of Kansas, Lawrence, USA

A. Al-bataineh, P. Baringer, A. Bean, J.F. Benitez, S. Boren, J. Bowen, J. Castle, S. Khalil, A. Kropivnitskaya, D. Majumder, W. Mcbrayer, M. Murray, C. Rogan, C. Royon, S. Sanders, E. Schmitz, J.D. Tapia Takaki, Q. Wang

Kansas State University, Manhattan, USA

A. Ivanov, K. Kaadze, Y. Maravin, A. Modak, A. Mohammadi, L.K. Saini, N. Skhirtladze

Lawrence Livermore National Laboratory, Livermore, USA

F. Rebassoo, D. Wright

University of Maryland, College Park, USA

A. Baden, O. Baron, A. Belloni, S.C. Eno, Y. Feng, C. Ferraioli, N.J. Hadley, S. Jabeen, G.Y. Jeng, R.G. Kellogg, J. Kunkle, A.C. Mignerey, F. Ricci-Tam, Y.H. Shin, A. Skuja, S.C. Tonwar

Massachusetts Institute of Technology, Cambridge, USA

D. Abercrombie, B. Allen, V. Azzolini, R. Barbieri, A. Baty, G. Bauer, R. Bi, S. Brandt, W. Busza, I.A. Cali, M. D'Alfonso, Z. Demiragli, G. Gomez Ceballos, M. Goncharov, P. Harris, D. Hsu, M. Hu, Y. Iiyama, G.M. Innocenti, M. Klute, D. Kovalskyi, Y.-J. Lee, A. Levin, P.D. Luckey, B. Maier, A.C. Marini, C. McGinn, C. Mironov, S. Narayanan, X. Niu, C. Paus, C. Roland, G. Roland, G.S.F. Stephans, K. Sumorok, K. Tatar, D. Velicanu, J. Wang, T.W. Wang, B. Wyslouch, S. Zhaozhong

University of Minnesota, Minneapolis, USA

A.C. Benvenuti, R.M. Chatterjee, A. Evans, P. Hansen, S. Kalafut, Y. Kubota, Z. Lesko, J. Mans, S. Nourbakhsh, N. Ruckstuhl, R. Rusack, J. Turkewitz, M.A. Wadud

University of Mississippi, Oxford, USA

J.G. Acosta, S. Oliveros

University of Nebraska-Lincoln, Lincoln, USA

E. Avdeeva, K. Bloom, D.R. Claes, C. Fangmeier, F. Golf, R. Gonzalez Suarez, R. Kamalieddin, I. Kravchenko, J. Monroy, J.E. Siado, G.R. Snow, B. Stieger

State University of New York at Buffalo, Buffalo, USA

A. Godshalk, C. Harrington, I. Iashvili, D. Nguyen, A. Parker, S. Rappoccio, B. Roozbahani

Northeastern University, Boston, USA

G. Alverson, E. Barberis, C. Freer, A. Hortiangtham, A. Massironi, D.M. Morse, T. Orimoto, R. Teixeira De Lima, T. Wamorkar, B. Wang, A. Wisecarver, D. Wood

Northwestern University, Evanston, USA

S. Bhattacharya, O. Charaf, K.A. Hahn, N. Mucia, N. Odell, M.H. Schmitt, K. Sung, M. Trovato, M. Velasco

University of Notre Dame, Notre Dame, USA

R. Bucci, N. Dev, M. Hildreth, K. Hurtado Anampa, C. Jessop, D.J. Karmgard, N. Kellams, K. Lannon, W. Li, N. Loukas, N. Marinelli, F. Meng, C. Mueller, Y. Musienko³⁹, M. Planer, A. Reinsvold, R. Ruchti, P. Siddireddy, G. Smith, S. Taroni, M. Wayne, A. Wightman, M. Wolf, A. Woodard

The Ohio State University, Columbus, USA

J. Alimena, L. Antonelli, B. Bylsma, L.S. Durkin, S. Flowers, B. Francis, A. Hart, C. Hill, W. Ji, T.Y. Ling, W. Luo, B.L. Winer, H.W. Wulsin

Princeton University, Princeton, USA

S. Cooperstein, O. Driga, P. Elmer, J. Hardenbrook, P. Hebda, S. Higginbotham, A. Kalogeropoulos, D. Lange, J. Luo, D. Marlow, K. Mei, I. Ojalvo, J. Olsen, C. Palmer, P. Piroué, J. Salfeld-Nebgen, D. Stickland, C. Tully

University of Puerto Rico, Mayaguez, USA

S. Malik, S. Norberg

Purdue University, West Lafayette, USA

A. Barker, V.E. Barnes, S. Das, L. Gutay, M. Jones, A.W. Jung, A. Khatiwada, D.H. Miller, N. Neumeister, C.C. Peng, H. Qiu, J.F. Schulte, J. Sun, F. Wang, R. Xiao, W. Xie

Purdue University Northwest, Hammond, USA

T. Cheng, J. Dolen, N. Parashar

Rice University, Houston, USA

Z. Chen, K.M. Ecklund, S. Freed, F.J.M. Geurts, M. Guilbaud, M. Kilpatrick, W. Li, B. Michlin, B.P. Padley, J. Roberts, J. Rorie, W. Shi, Z. Tu, J. Zabel, A. Zhang

University of Rochester, Rochester, USA

A. Bodek, P. de Barbaro, R. Demina, Y.t. Duh, T. Ferbel, M. Galanti, A. Garcia-Bellido, J. Han, O. Hindrichs, A. Khukhunaishvili, K.H. Lo, P. Tan, M. Verzetti

The Rockefeller University, New York, USA

R. Ciesielski, K. Goulianos, C. Mesropian

Rutgers, The State University of New Jersey, Piscataway, USA

A. Agapitos, J.P. Chou, Y. Gershtein, T.A. Gómez Espinosa, E. Halkiadakis, M. Heindl, E. Hughes, S. Kaplan, R. Kunnawalkam Elayavalli, S. Kyriacou, A. Lath, R. Montalvo, K. Nash, M. Osherson, H. Saka, S. Salur, S. Schnetzer, D. Sheffield, S. Somalwar, R. Stone, S. Thomas, P. Thomassen, M. Walker

University of Tennessee, Knoxville, USA

A.G. Delannoy, J. Heideman, G. Riley, K. Rose, S. Spanier, K. Thapa

Texas A&M University, College Station, USA

O. Bouhali⁷⁵, A. Castaneda Hernandez⁷⁵, A. Celik, M. Dalchenko, M. De Mattia, A. Delgado, S. Dildick, R. Eusebi, J. Gilmore, T. Huang, T. Kamon⁷⁶, R. Mueller, Y. Pakhotin, R. Patel, A. Perloff, L. Perniè, D. Rathjens, A. Safonov, A. Tatarinov

Texas Tech University, Lubbock, USA

N. Akchurin, J. Damgov, F. De Guio, P.R. Duderov, J. Faulkner, E. Gurpinar, S. Kunori,

K. Lamichhane, S.W. Lee, T. Mengke, S. Muthumuni, T. Peltola, S. Undleeb, I. Volobouev, Z. Wang

Vanderbilt University, Nashville, USA

S. Greene, A. Gurrola, R. Janjam, W. Johns, C. Maguire, A. Melo, H. Ni, K. Padeken, J.D. Ruiz Alvarez, P. Sheldon, S. Tuo, J. Velkovska, Q. Xu

University of Virginia, Charlottesville, USA

M.W. Arenton, P. Barria, B. Cox, R. Hirosky, M. Joyce, A. Ledovskoy, H. Li, C. Neu, T. Sinthuprasith, Y. Wang, E. Wolfe, F. Xia

Wayne State University, Detroit, USA

R. Harr, P.E. Karchin, N. Poudyal, J. Sturdy, P. Thapa, S. Zaleski

University of Wisconsin - Madison, Madison, WI, USA

M. Brodski, J. Buchanan, C. Caillol, D. Carlsmith, S. Dasu, L. Dodd, S. Duric, B. Gomber, M. Grothe, M. Herndon, A. Hervé, U. Hussain, P. Klabbers, A. Lanaro, A. Levine, K. Long, R. Loveless, V. Rekovic, T. Ruggles, A. Savin, N. Smith, W.H. Smith, N. Woods

†: Deceased

1: Also at Vienna University of Technology, Vienna, Austria

2: Also at IRFU, CEA, Université Paris-Saclay, Gif-sur-Yvette, France

3: Also at Universidade Estadual de Campinas, Campinas, Brazil

4: Also at Federal University of Rio Grande do Sul, Porto Alegre, Brazil

5: Also at Universidade Federal de Pelotas, Pelotas, Brazil

6: Also at Université Libre de Bruxelles, Bruxelles, Belgium

7: Also at Institute for Theoretical and Experimental Physics, Moscow, Russia

8: Also at Joint Institute for Nuclear Research, Dubna, Russia

9: Also at Cairo University, Cairo, Egypt

10: Also at Helwan University, Cairo, Egypt

11: Now at Zewail City of Science and Technology, Zewail, Egypt

12: Also at British University in Egypt, Cairo, Egypt

13: Now at Ain Shams University, Cairo, Egypt

14: Also at Department of Physics, King Abdulaziz University, Jeddah, Saudi Arabia

15: Also at Université de Haute Alsace, Mulhouse, France

16: Also at Skobeltsyn Institute of Nuclear Physics, Lomonosov Moscow State University, Moscow, Russia

17: Also at Tbilisi State University, Tbilisi, Georgia

18: Also at CERN, European Organization for Nuclear Research, Geneva, Switzerland

19: Also at RWTH Aachen University, III. Physikalisches Institut A, Aachen, Germany

20: Also at University of Hamburg, Hamburg, Germany

21: Also at Brandenburg University of Technology, Cottbus, Germany

22: Also at Institute of Nuclear Research ATOMKI, Debrecen, Hungary

23: Also at MTA-ELTE Lendület CMS Particle and Nuclear Physics Group, Eötvös Loránd University, Budapest, Hungary

24: Also at Institute of Physics, University of Debrecen, Debrecen, Hungary

25: Also at Indian Institute of Technology Bhubaneswar, Bhubaneswar, India

26: Also at Institute of Physics, Bhubaneswar, India

27: Also at Shoolini University, Solan, India

28: Also at University of Visva-Bharati, Santiniketan, India

29: Also at University of Ruhuna, Matara, Sri Lanka

30: Also at Isfahan University of Technology, Isfahan, Iran

- 31: Also at Yazd University, Yazd, Iran
- 32: Also at Plasma Physics Research Center, Science and Research Branch, Islamic Azad University, Tehran, Iran
- 33: Also at Università degli Studi di Siena, Siena, Italy
- 34: Also at INFN Sezione di Milano-Bicocca ^a, Università di Milano-Bicocca ^b, Milano, Italy
- 35: Also at International Islamic University of Malaysia, Kuala Lumpur, Malaysia
- 36: Also at Malaysian Nuclear Agency, MOSTI, Kajang, Malaysia
- 37: Also at Consejo Nacional de Ciencia y Tecnología, Mexico City, Mexico
- 38: Also at Warsaw University of Technology, Institute of Electronic Systems, Warsaw, Poland
- 39: Also at Institute for Nuclear Research, Moscow, Russia
- 40: Now at National Research Nuclear University 'Moscow Engineering Physics Institute' (MEPhI), Moscow, Russia
- 41: Also at St. Petersburg State Polytechnical University, St. Petersburg, Russia
- 42: Also at University of Florida, Gainesville, USA
- 43: Also at P.N. Lebedev Physical Institute, Moscow, Russia
- 44: Also at California Institute of Technology, Pasadena, USA
- 45: Also at Budker Institute of Nuclear Physics, Novosibirsk, Russia
- 46: Also at Faculty of Physics, University of Belgrade, Belgrade, Serbia
- 47: Also at INFN Sezione di Pavia ^a, Università di Pavia ^b, Pavia, Italy
- 48: Also at University of Belgrade, Faculty of Physics and Vinca Institute of Nuclear Sciences, Belgrade, Serbia
- 49: Also at Scuola Normale e Sezione dell'INFN, Pisa, Italy
- 50: Also at National and Kapodistrian University of Athens, Athens, Greece
- 51: Also at Riga Technical University, Riga, Latvia
- 52: Also at Universität Zürich, Zurich, Switzerland
- 53: Also at Stefan Meyer Institute for Subatomic Physics (SMI), Vienna, Austria
- 54: Also at Adiyaman University, Adiyaman, Turkey
- 55: Also at Istanbul Aydin University, Istanbul, Turkey
- 56: Also at Mersin University, Mersin, Turkey
- 57: Also at Piri Reis University, Istanbul, Turkey
- 58: Also at Izmir Institute of Technology, Izmir, Turkey
- 59: Also at Necmettin Erbakan University, Konya, Turkey
- 60: Also at Marmara University, Istanbul, Turkey
- 61: Also at Kafkas University, Kars, Turkey
- 62: Also at Istanbul Bilgi University, Istanbul, Turkey
- 63: Also at Rutherford Appleton Laboratory, Didcot, United Kingdom
- 64: Also at School of Physics and Astronomy, University of Southampton, Southampton, United Kingdom
- 65: Also at Monash University, Faculty of Science, Clayton, Australia
- 66: Also at Instituto de Astrofísica de Canarias, La Laguna, Spain
- 67: Also at Bethel University, St. Paul, USA
- 68: Also at Utah Valley University, Orem, USA
- 69: Also at Purdue University, West Lafayette, USA
- 70: Also at Beykent University, Istanbul, Turkey
- 71: Also at Bingol University, Bingol, Turkey
- 72: Also at Erzincan University, Erzincan, Turkey
- 73: Also at Sinop University, Sinop, Turkey
- 74: Also at Mimar Sinan University, Istanbul, Istanbul, Turkey
- 75: Also at Texas A&M University at Qatar, Doha, Qatar

76: Also at Kyungpook National University, Daegu, Korea